Journal of Rock Mechanics and Geotechnical Engineering 17 (2025) 1302–1320

Contents lists available at ScienceDirect

Journal of Rock Mechanics and Geotechnical Engineering

journal homepage: www.jrmge.cn

Full Length Article

Confined seepage analysis of saturated soils using fuzzy fields

Nataly A. Manque [a, *], Kok-Kwang Phoon [b], Yong Liu [c], Marcos A. Valdebenito [a], Matthias G.R. Faes [a]

[a] Reliability Engineering, TU Dortmund University, Dortmund, 44227, Germany
[b] Singapore University of Technology and Design, Singapore, 487372, Singapore
[c] State Key Laboratory of Water Resources Engineering and Management, Wuhan University, Wuhan, 430072, China

ARTICLE INFO

Article history:
Received 16 November 2023
Received in revised form
19 July 2024
Accepted 31 July 2024
Available online 17 October 2024

Keywords:
Fuzzy fields
Interval fields
Seepage analysis
Hydraulic conductivity
Spatial uncertainty

ABSTRACT

Seepage refers to the flow of water through porous materials. This phenomenon has a crucial role in dam, slope, excavation, tunnel, and well design. Performing seepage analysis usually is a challenging task, as one must cope with the uncertainty associated with the parameters such as the hydraulic conductivity in the horizontal and vertical directions that drive this phenomenon. However, at the same time, the data on horizontal and vertical hydraulic conductivities are typically scarce in spatial resolution. In this context, so-called non-traditional approaches for uncertainty quantification (such as intervals and fuzzy variables) offer an interesting alternative to classical probabilistic methods, since they have been shown to be quite effective when limited information on the governing parameters of a phenomenon is available. Therefore, the main contribution of this study is the development of a framework for conducting seepage analysis in saturated soils, where uncertainty associated with hydraulic conductivity is characterized using fuzzy fields. This method to characterize uncertainty extends interval fields towards the domain of fuzzy numbers. In fact, it is illustrated that fuzzy fields are an effective tool for capturing uncertainties with a spatial component, since they allow one to account for available physical measurements. A case study in confined saturated soil shows that with the proposed framework, it is possible to quantify the uncertainty associated with seepage flow, exit gradient, and uplift force effectively.

1. Introduction

Seepage analysis plays a significant role in practical engineering problems such as the design of dams and hydraulic structures (Jie et al., 2013), reservoirs (Li et al., 2020), embankments (Liu et al., 2017a), underground spaces (Wang, 2021), railway ballasts (Alrdadi and Meylan, 2022), tunnels (Wang et al., 2021), and the analysis of rainfall-induced landslides (Cai et al., 2017). Seepage analyses have been carried out using analytical methods such as flow nets, and numerical methods such as the finite element method (FEM), the finite difference method (FDM), and the boundary element method (BEM) (Li et al., 2020). The seepage phenomenon obeys Darcy's law, and it is governed by the hydraulic conductivity, the piezometric head, and boundary conditions such as specified heads and fluxes, under saturated steady-state conditions (Richards, 1931; Phoon et al., 2010). Saturated seepage, which describes the phenomenon of water percolating through the pores of the soil when the surrounding material is fully saturated, is commonly used in the design of dams and reservoirs where large volumes of water are involved, and in foundation projects where the ground is fully saturated (Hager et al., 2020). Among the parameters that govern seepage in saturated soils, hydraulic conductivity is particularly challenging to characterize due to significant soil uncertainty (Santoso et al., 2011). Thus, this imposes a major obstacle for performing seepage analysis accurately (Le et al., 2011; Phoon, 2019).

Several assumptions concerning hydraulic conductivity are included in the standard procedure for dealing with seepage problems. Deterministic analyses that consider hydraulic conductivity values from handbooks are usually applied. Nevertheless, this practice can lead to inaccuracies in the hydraulic conductivity characterization, due to the lack, scarcity, and imprecision of available data (Phoon and Kulhawy, 1999). Geologic processes that have created and continuously altered soil mass do not necessarily ensure that hydraulic conductivity values collected in one area are

* Corresponding author.
E-mail address: nataly.manque@tu-dortmund.de (N.A. Manque).
Peer review under responsibility of Institute of Rock and Soil Mechanics, Chinese Academy of Sciences.

https://doi.org/10.1016/j.jrmge.2024.07.016

valid in soils of the same classification in other areas (Dane and Topp, 2002). Furthermore, deterministic seepage analyses are usually performed under the assumption of homogeneous behavior of the soil (Shedid, 2019). However, soil properties, especially hydraulic conductivity, exhibit considerable heterogeneity at different spatial scales in conjunction with complex interactions with environmental conditions (Lin, 2010; Baroni et al., 2017).

Despite the existence of techniques to measure the hydraulic conductivity in the field (Elhakim, 2016), hydraulic conductivity quantification can be affected by the spatial variability of the soil (Baroni et al., 2017), as well as inaccuracy and sparseness of the field measurements (Guan and Wang, 2022). Therefore, uncertainty in hydraulic conductivity can be attributed to two causes. First, the quantification is affected by the inherent uncertainty of the soil (Phoon and Kulhawy, 1999) which is a consequence of many factors, such as the void ratio and mineralogy (Teng et al., 2019), size, shape, packing, and orientation of soil grains (Deng et al., 2011), pore size distribution of the soil mass, and pore interconnection (Zeng et al., 2020). Second, the quantification is also affected by the scatter and error of the measurement data. Whereas databases containing data collected from various locations are available (Feng and Vardanega, 2019), site-specific data are limited. In a typical project, only a limited number of soil samples are extracted from a few boreholes. Therefore, the hydraulic conductivity is known only for a small number of positions, whereas for the remaining positions, hydraulic conductivity values must be estimated from the borehole measurements (Gong et al., 2020). Furthermore, significant differences can be observed by comparing the results of different tests. The work of Elhakim (2016) recorded values of hydraulic conductivity obtained from different methods that exhibited a coefficient of variation as high as 240% in the same soil layer. Consequently, an accurate quantification of hydraulic conductivity is required to accurately estimate seepage performance, that accounts for both sources of uncertainty: the spatial variability of the soil and the imprecision and sparseness of field measurements.

It was not until the pioneering study by Griffiths and Fenton (1993) that hydraulic conductivity was incorporated into seepage analysis in a non-deterministic manner. Based on this study, the uncertainty in hydraulic conductivity has been incorporated from different perspectives in seepage problems, using probabilistic and possibilistic approaches. Probabilistic analysis of saturated and unsaturated steady-state seepage has been applied widely, e.g. Griffiths and Fenton (1997), Ahmed (2009), Srivastava et al. (2010), and Sharma et al. (2021). In these approaches, hydraulic conductivity is treated as a random field (Santoso et al., 2010, 2011), while assuming a homogeneous soil layer, isotropic soil behavior, and autocorrelation functions in most cases. Spatial variation in the hydraulic conductivity has also been accounted for by applying non-stationary random fields for stochastic analyses in Cho (2012) and Liu et al. (2017a). Nevertheless, spatial dependencies have been included using theoretical autocorrelation functions, that did not consider field measurements in their definition, due to the scarcity of available data (Montoya-Noguera et al., 2019). Techniques that allow the incorporation of site-specific data, such as conditional simulation methods, have been used to constrain the spatial distribution of soil parameters to the real data for slope reliability analysis (Jiang et al., 2022). In contrast, very few applications of possibilistic methods (Beer et al., 2013a) have been developed for seepage analysis. An example is the affine arithmetic analysis applied in Degrauwe et al. (2010) for estimating groundwater flow under a dam. Here, the same nominal value and interval range for vertical and horizontal hydraulic conductivity were considered. Another technique within the non-probabilistic methods corresponds to interval fields (Faes and Moens, 2017). Interval fields are an extension of the interval framework (Moore, 1966) when uncertainty is influenced by physical space (Sofi et al., 2019). This technique is arguably more reasonable in the presence of scarce measurements of uncertain properties. This is because when the lack of information is particularly pronounced, it raises concerns about the ability to specify a probabilistic model for specific parameters (Beer et al., 2013b). In addition, the potential limitations of a probabilistic approach in dealing with limited data have recently been highlighted by the application of imprecise probabilities in geotechnical engineering. For example, distribution-free P-boxes provide a robust and consistent way to represent uncertainty when data are scarce. They provide bounds on the possible cumulative distribution function (CDF) without relying on specific distribution assumptions. The work of Faes et al. (2022) shows that in case of high uncertainty in a geotechnical context, an interval approach is more appropriate than, for example, assuming a certain distribution, especially in cases where the tails of the distribution are not adequately captured. To the best of our knowledge, there are few applications of interval fields to deal with the uncertainty of hydraulic conductivity. The work reported in Verhaeghe et al. (2013) shows an application of interval fields to a geohydrological problem in which the transport of solutes in groundwater is solved considering an uncertain saturated hydraulic conductivity. The work reported in Feng et al. (2022) also used interval fields, but this contribution focused on slope stability instead of seepage flow. Fuzzy set theory has also been applied to seepage analysis (Zhang et al., 2020, 2022). Nevertheless, these applications have focused on the use of fuzzy numbers to incorporate uncertainty in reservoir properties, disregarding the spatial component in soil properties such as hydraulic conductivity. Therefore, the challenge remains to develop strategies for seepage analysis that consider available physical measurements while considering the effects of spatial uncertainty.

Under such a scenario, this study presents a methodology for conducting seepage analysis in saturated soils using a fuzzy approach. This method is chosen due to its inherent advantages over stochastic methods when dealing with limited and uncertain input data. The adoption of a possibilistic methodology enables the characterization of uncertain parameters by simply specifying the range of possible values for each parameter, i.e. only the bounds of each of them are required. Moreover, it is not necessary to assume the marginal distribution and correlation functions of the input data. Geostatistical methods, such as semi variograms and correlation functions that are essential for Kriging modeling, facilitate the identification of spatial dependencies within data sets. Nevertheless, their effectiveness depends on the availability of large data sets that are typically both reasonably dense and homogeneously distributed across the spatial domain (Hesse et al., 2024). In contrast, interval-based approaches provide a more flexible framework for dealing with spatial uncertainty by requiring comparatively less data. Furthermore, possibilistic methods have shown considerable potential under severe uncertainty, especially when their source stems from scarcity and inaccuracy of data (Faes et al., 2019; Schietzold et al., 2019). Specifically, the proposed methodology extends the interval field theory to fuzzy analysis. For constructing the basis functions related to the interval field, only one parameter needs to be selected. This parameter corresponds to the exponent of the distance measure considered, which governs the influence of the available information at specific locations on the domain over the rest of the field. As a result, utilizing interval fields facilitates the incorporation of sparse spatial information, while extending to fuzzy techniques allows for sensitivity inclusion in the seepage analysis.

Therefore, the objective of this work is to explore the application of fuzzy fields (Verhaeghe et al., 2010, 2013) as a means for characterizing uncertainty in seepage analysis. This is a novel

contribution when compared to existing approaches reported in the literature (Santoso et al., 2011; Liu et al., 2017a; Sharma et al., 2021), which can be particularly useful when data measurements are scarce. In this context, fuzzy fields are defined as a natural extension of interval fields. This is achieved by defining the interval fields in a fuzzy sense to assess the sensitivity of the predicted spatial bounds of the uncertain parameters towards the input uncertainty. Specifically, the fuzzy fields are defined based on an extension of the Inverse Distance Weighting framework that is commonly used to construct the required interval field basis functions (Faes and Moens, 2017). Concerning the propagation of the fuzzy field, the traditional alpha-level optimization strategy is adopted for calculating the membership function associated with seepage responses in a discrete manner (Möller et al., 2000; Hanss, 2005). A numerical example illustrates that the proposed strategy allows for accurately characterizing the fuzzy seepage flow, uplift force, and exit gradient.

It is emphasized that this work addresses the confined saturated seepage problem to focus on the treatment of spatial uncertainty in soil properties under limited data. Note that the term spatial uncertainty is used in this work to consider uncertainty in its widest form. This means that not only the intrinsic spatial uncertainty of the soil is considered, but also the potential lack of knowledge that exists, stemming from scarcity in measurement data. Given the focus of this work on spatial uncertainty, other relevant cases of seepage analysis are not considered for the sake of simplicity. For example, the analysis of unsaturated seepage (Zhai and Rahardjo, 2013; Prakash et al., 2021), which is crucial for the study of e.g. irrigation canals and drainage systems (Huang and Jia, 2009), groundwater containment systems (Abd-Elaty et al., 2019), and rainfall-induced landslides (Gu et al., 2023) (among others), is not addressed due to the challenges associated with the resulting numerical models, which are costly to solve numerically (Bianchi et al., 2022). The latter is particularly true in the context of uncertainty quantification, where these numerical models need to be solved repeatedly.

The structure of the remaining sections of the paper is as follows. The formulation of the seepage problem considered in this paper and the spatial component of hydraulic conductivity uncertainty are discussed in Section 2. Section 3 introduces the fundamentals of interval and fuzzy field theory. Here, the proposed strategy for performing seepage analysis with fuzzy fields is discussed, while its application is illustrated and analyzed by means of an example in Section 4. Conclusions are summarized in Section 5.

2. Seepage analysis

2.1. Governing equations

The partial differential equation that governs the two-dimensional (2D) steady-state confined seepage problem is

$$\frac{\partial}{\partial x}\left(k_{\mathrm{H}}\frac{\partial h}{\partial x}\right)+\frac{\partial}{\partial y}\left(k_{\mathrm{V}}\frac{\partial h}{\partial y}\right)=0 \tag{1}$$

where k_{H} and k_{V} correspond to the horizontal and vertical hydraulic conductivities, respectively; h is the hydraulic head; x and y are the Cartesian coordinates of the domain Ω. Eq. (1) is a variant of Richards' equation (Richards, 1931), which was derived on the assumption that saturated flow obeys Darcy's law. Eq. (1) is typically solved in a discrete manner by means of the FEM:

$$\boldsymbol{K}\boldsymbol{h}=\boldsymbol{q} \tag{2}$$

where $\boldsymbol{K}\in\mathbb{R}^{n_d\times n_d}$ is the matrix associated with the soil hydraulic conductivity; $\boldsymbol{q}\in\mathbb{R}^{n_d\times 1}$ is the vector representing nodal flow; and $\boldsymbol{h}\in\mathbb{R}^{n_d\times 1}$ is the vector that describes the system's response, that is, hydraulic head. The quantity n_d corresponds to the degrees-of-freedom considered. The model described by Eqs. (1) and (2) corresponds to the classical deterministic approach for dealing with seepage problems. After solving Eq. (2), quantities associated with the seepage phenomenon such as flow, uplift force, and exit gradients can be readily derived.

2.2. Spatial variation of hydraulic conductivity

Hydraulic conductivity is the property of a soil that permits water or any liquid to flow through its voids (Whitlow, 2000). For a 2D flow, horizontal hydraulic conductivity k_{H} is the hydraulic conductivity for flow perpendicular to gravity. Conversely, the vertical hydraulic conductivity k_{V} is the hydraulic conductivity for flow in the direction aligned with the direction of the gravity field (Fanchi, 2010). Hydraulic conductivity can be estimated based on field measurements from different methods. Pumping tests provide a good estimation for the representative hydraulic conductivity in a soil layer (Elhakim, 2016). The hydraulic conductivity is estimated indirectly using the transmissibility of the saturated soil thickness (Ahmed et al., 2008). Piezocone tests (commonly known as CPTu) are another useful tool for estimating hydraulic conductivity as a function of pore pressure dissipation measured at different depths (Eslami et al., 2019). Use of the falling head test in boreholes allows for evaluation of the hydraulic conductivity of the soil layer being investigated, by measuring the water depth inside the casing at specific time intervals (Xiang et al., 1997). All these methods provide, directly or indirectly, spatially distributed hydraulic conductivity measurements. Nevertheless, it is noteworthy that these techniques are rather high-cost and, consequently, their applicability cannot be extended to most projects (Singh et al., 2020). Hence, the values measured at a specific depth in a small fraction of the soil are considered representative of all soil layers in traditional seepage analysis, not fully including the heterogeneous behavior of the soil. Vertical hydraulic conductivity can be measured in the laboratory or in pressure transient tests in the field (Ahmed et al., 2008; Elhakim, 2016). In many cases, vertical hydraulic conductivity is not measured, since it is very complex, expensive, and time-consuming. For those reasons, normally k_{V} must be assumed from horizontal hydraulic conductivity measurements. As a rule of thumb, the vertical hydraulic conductivity is about one-tenth of the horizontal hydraulic conductivity (Fanchi, 2010). Depending on the type of soil or rock, occurrence of fractures, voids, and porosity of the medium, both hydraulic conductivities can become equal (Shedid, 2019).

The anisotropy governing hydraulic conductivity has its origin in the heterogeneity of the soil. Soil regions, whether in natural or compacted soils, are often characterized by a high degree of spatial heterogeneity due to geomorphological processes or deficient building control in earth structures (Cho, 2012). The large fluctuations of hydraulic conductivity values recorded in the literature even for one layer and the wide ranges typically suggested by soil type indicate this heterogeneity of hydraulic conductivity. Spatial variations influencing hydraulic conductivity values can appear at different scales. Variations can be evidenced at very slight distances, due to changes in soil grain size and shape (Deng et al., 2011). Similarly, variations on a larger scale may also be observed, for example, due to soil stratifications (Lu and Zhang, 2007). Thus, it is challenging to define hydraulic conductivity values for a soil region. Therefore, a key element to characterize hydraulic conductivity is to consider strategies that allow for spatial dependencies. To avoid the use of theoretical assumptions and where data are scarce, interval and fuzzy sets methods provide an appropriate

framework for dealing with such uncertainty in a non-probabilistic manner (Sofi et al., 2019).

3. Fuzzy fields

3.1. General remarks

The nature of hydraulic conductivity outlined in the preceding section highlights that, for an accurate analysis of seepage, hydraulic conductivity must be regarded as uncertain. Therefore, Eq. (2) can be rewritten as

$$\boldsymbol{K}(\xi)\boldsymbol{h}(\xi) = \boldsymbol{q}(\xi) \tag{3}$$

where ξ represents uncertainty in hydraulic conductivity. Specifically, ξ represents the horizontal and vertical hydraulic conductivities in the seepage problem, which, unlike the deterministic approach shown in Eqs. (1) and (2), do not correspond to fixed values. The approach used to represent ξ in this study is described in Section 3.3.2. The intrinsic nature of the hydraulic conductivity of the soil makes it necessary to include its uncertainty when defining the properties of the system. Therefore, the matrix associated with the soil hydraulic conductivity $\boldsymbol{K}(\xi)$ will depend on the uncertainty. This uncertainty, which is captured in the variable ξ, is constructed using the available hydraulic conductivity information. This process is explained in detail in the following subsections. Thus, ξ allows one to incorporate the physical and spatial nature of the hydraulic conductivity of the soil as well as its uncertainty. As can be seen from Eq. (3), the uncertainty affecting the hydraulic conductivity matrix $\boldsymbol{K}(\xi)$ is propagated to the hydraulic head $\boldsymbol{h}(\xi)$ and the flow $\boldsymbol{q}(\xi)$. This is due to the propagation of uncertainty that occurs during the modeling phase. Hence, the necessity to quantify the uncertainty in the responses of interest of the model (such as seepage flow, uplift force, and exit gradients) arises.

In this work, a possibilistic approach is considered to quantify the uncertainty in hydraulic conductivity. Within the possibilistic approaches, there are several methods to describe uncertainty (Beer et al., 2013a), that is, to define ξ. One way is to resort to interval methods (Moens and Vandepitte, 2007). Interval methods are very convenient in cases where there is imprecise knowledge of a given variable and just its boundary values can be defined (Imholz et al., 2020). Interval fields (Faes and Moens, 2017) are a generalization of interval methods, which allows for spatial dependence to be incorporated. For this purpose, a set of functions are used to describe the effect of spatial coordinates on the uncertain property. Both techniques, interval, and interval fields are discussed in Section 3.2. A further category of possibilistic methods corresponds to fuzzy approaches (Möller et al., 2000). These techniques are described in Section 3.3. Among them, a fuzzy variable can be interpreted as a collection of intervals indexed by a membership function. This approach to describe uncertain parameters can be extended to fuzzy fields (Schietzold et al., 2019) in the same way that intervals can be extended to interval fields, considering that there is spatial dependence. Some applications of fuzzy fields can be found in the literature. Verhaeghe et al. (2013) has presented a study of solute transport in groundwater pollution problem using spatial fuzzy numbers, and Götz et al. (2019) has analyzed unknown environmental conditions and loading scenarios on an asphalt structure considering dependencies in fuzzy analysis.

The use of a possibility-based approach to seepage analysis is complementary to probabilistic methods such as random field analysis (Vanmarcke, 1983). Intervals (fields) are particularly useful when dealing with severe uncertainties where spatial data may be limited in both quantity and quality (Faes et al., 2019). While probabilistic approaches are well suited when sufficient data are available, they may not be appropriate in scenarios with sparse data and limited knowledge, such as uncertainties in soil properties. This is because they are very likely to underestimate the worst-case behavior of the structure (Beer et al., 2013b). The reasons for insufficient data to support probabilistic methods are diverse and include the challenges of collecting statistical data for large-scale systems, as well as the inherent complexity and cost associated with obtaining such data (He et al., 2007), being the latter particularly noticeable for variables such as hydraulic conductivity, as discussed in Section 2.2. Therefore, non-probabilistic methods are considered to provide a more objective and accurate quantification of uncertainty when data are either vague or scarce (Faes et al., 2019). In addition, unlike random fields, non-probabilistic approaches such as interval or fuzzy analysis require fewer assumptions in characterizing uncertain parameters. There is no need to assume specific marginal distributions or autocorrelation functions. Instead, only the range of plausible values for these uncertain parameters needs to be defined, a task that can be accomplished even with sparse data. Moreover, when using interval fields, the only parameter that needs to be defined is the exponent used for the distance measure of the basis functions, a concept which is elaborated in Sections 3.2.2 and 4.5. Furthermore, the use of fuzzy techniques enables sensitivity analysis (Möller and Beer, 2004). This advantage provides a comprehensive analysis of uncertainties while minimizing the assumptions required in the modeling process when combined with interval methods.

Once uncertainty in hydraulic conductivity is described, it becomes necessary to propagate this uncertainty to the quantities of interest (seepage flow, uplift force, and exit gradients) considering spatial dependencies. It is crucial to emphasize that in cases where non-probabilistic methods are used, traditional statistical indicators such as mean, standard deviation, and coefficient of variation are not applicable to characterize the uncertain responses of the system. Instead, when using intervals and interval fields, the response of the system is represented as an interval, whereas in fuzzy approaches the response is characterized by a membership function. Furthermore, when interval fields are used to characterize uncertainty, the correlation concept is replaced by the dependence concept (Faes and Moens, 2020). Within the different existing methods for propagating uncertainty, i.e. to obtain the system's response, the traditional alpha-level optimization strategy (Möller et al., 2000) is adopted in this study to estimate the membership function associated with the seepage responses in a discrete manner. This methodology is presented in Section 3.4. The analysis of these responses also differs from the traditional approach when it comes to decision-making, as it is obtained from a non-probabilistic approach. The membership functions must be analyzed in their discrete form, that is, by the intervals associated with different membership levels. This approach allows the user to gain insight into the range or extent of the interval that contains each possible value for the response being analyzed. It also gives an idea of the effect of uncertainty in the input parameters and how the sensitivity of the response relates to the membership level being considered. As a result, users can get feedback on the effect of the chosen characterization of the uncertain parameters, improving the comprehensibility and robustness of the analysis. Furthermore, when it comes to making critical engineering decisions, one of the key attributes of interval analysis is its remarkable focus on extreme events. This is particularly advantageous when dealing with risk assessments involving rare, high-consequence events (Beer et al., 2013b).

3.2. Interval approaches

3.2.1. Intervals

Interval methods have been widely used to estimate the response of engineering systems (Degrauwe et al., 2010; Faes and Moens, 2019a). By definition, an interval ξ^I corresponds to a set of possible values that the physical variable ξ is allowed to assume, which are bounded by a lower and an upper limit, that is $\xi \in \left[\underline{\xi}, \overline{\xi}\right]$. Therefore, this strategy allows an uncertain variable ξ to be represented by a closed finite interval. Interval analysis is an interesting technique when limited information is available (Faes and Moens, 2019a). Nevertheless, when the uncertain variable is space-dependent, this approach must be extended to capture such behavior, as discussed below.

3.2.2. Interval fields

Interval fields are a natural extension of the concept of interval whenever uncertainty is influenced by space location (Sofi et al., 2019). To define an interval field, consider that the spatial domain associated with the interval field is denoted as Ω and a spatial coordinate within that domain is denoted by means of vector $\boldsymbol{x}$, thus $\boldsymbol{x} \in \Omega$. It is assumed that there are a few n_b locations within Ω at which field measurements are available. The aforementioned locations are termed as control points and their positions are denoted as $\boldsymbol{x}_j$, with $j = 1,\ldots,n_b$. Observe that the dimension of the vector $\boldsymbol{x}_j$ is equal to the number of dimensions involved in the study. For simplicity, these positions are stored as columns of the matrix $\boldsymbol{X}$, that is, $\boldsymbol{X} = [\boldsymbol{x}_1, \ldots, \boldsymbol{x}_{n_b}]$. As there are field measurements at the control points, the uncertain property can be characterized as an interval, that is, $\xi_j \in \left[\underline{\xi}_j, \overline{\xi}_j\right]$, where ξ_j denotes the value of the uncertain property at the j-th control point. In other words, the interval associated with the uncertain property at location $\boldsymbol{x}_j$ is $\xi_j^I = \left[\underline{\xi}_j, \overline{\xi}_j\right]$. With these considerations, an interval field $\xi^I(\boldsymbol{x})$ is defined by

$$\xi^I(\boldsymbol{x}) = \sum_{j=1}^{n_b} \psi_j(\boldsymbol{x}, \boldsymbol{X}) \xi_j^I \tag{4}$$

where $\psi_j(\cdot,\cdot)$ denotes the basis functions that allow measuring the influence of the interval associated with the j-th control point on $\boldsymbol{x}$. It is important to note that the basis functions capture the spatial uncertainty in the domain Ω in patterns, yielding a mapping from the input domain into a reduced n_b −dimensional input space. Hence, the uncertainty present in a space-dependent property ξ is reduced to that contained in the intervals ξ_j^I associated with the n_b control points, as shown in Eq. (4). To illustrate this, Fig. 1 shows the interval field obtained when the property ξ is subject to spatial uncertainty. In this figure, two control points x_1 and x_2 are defined (that is, $n_b = 2$), which are located within the spatial domain Ω of the problem of interest. The top of Fig. 1 shows the lower $\underline{\xi}(x)$ and upper $\overline{\xi}(x)$ bounds of the resulting interval field. Note how interval fields yield an extension of the intervals known at certain locations to other positions where no measurements are available. It is noteworthy that, since for both control points an interval is defined, no assumption is made regarding the probability associated with certain values within these sets. To explain the role of the basis functions, see the bottom of Fig. 1, which shows the values of basis functions across the domain Ω. It follows from Eq. (4), that for an arbitrary location within the domain, it is possible to obtain the interval describing ξ by evaluating the value of the basis functions at that position. Note that the basis function $\psi_1(x)$ reaches value 1 for position x_1 and 0 for x_2, while for the basis function $\psi_2(x)$, the opposite is true.

The basis functions are defined in this work according to the following equation:

$$\psi_j(\boldsymbol{x}, \boldsymbol{X}) = \frac{w_j(\boldsymbol{x}, \boldsymbol{x}_j)}{\sum_{j_1=1}^{n_b} w_{j_1}\left(\boldsymbol{x}, \boldsymbol{x}_{j_1}\right)} \quad (j = 1, \ldots, n_b) \tag{5}$$

where $w_j(\boldsymbol{x}, \boldsymbol{x}_j)$ is the weight function between a specific spatial coordinate $\boldsymbol{x}$ and the control point $\boldsymbol{x}_j$. In this work, the weight functions w_j correspond to the inverse distance weighting function defined by

$$w_j(\boldsymbol{x}, \boldsymbol{x}_j) = \frac{1}{[d(\boldsymbol{x}, \boldsymbol{x}_j)]^p} \tag{6}$$

where $d(\boldsymbol{x}, \boldsymbol{x}_j)$ is the considered distance measure (e.g. Euclidean distance) between $\boldsymbol{x}$ and $\boldsymbol{x}_j$ and p is a positive real number. This parameter represents the influence that the information contained in the control point $\boldsymbol{x}_j$ is allowed to influence a given location $\boldsymbol{x}$ within the domain. Hence, a larger magnitude of p assigns a higher influence to values closer to $\boldsymbol{x}$. For the identification of the correct basis functions, Faes and Moens (2017) proposed to select a value for p that is low enough to interpolate the spatial uncertainty. Specifically, for problems in one and two dimensions, those authors note that using a value of $p = 2$ gives satisfactory results. In this contribution, the value of p is considered equal to 2 (van Mierlo et al., 2021). It is important to emphasize that Eq. (6) enables one to incorporate the physical anisotropy of the hydraulic conductivity, i.e. it allows the magnitudes of the conductivities to spatially vary within the domain. However, it does not allow for incorporating the effect that the vertical conductivity may fluctuate faster than the horizontal one.

Most commonly, hydraulic conductivity data are scarce when dealing with seepage problems, as discussed in Section 2.2. In such a scenario, the interval field approach described above is useful to incorporate scarce and uncertain spatial data. For that purpose, it is necessary to retrieve the hydraulic conductivity data at the control points, since the uncertainty associated with hydraulic conductivity is reduced to that existing at these locations, as shown in Eq. (4). To define the information at control points, field-measured data on hydraulic conductivity can be used. The location of each control point will be defined by the places where hydraulic conductivity was measured, for example, at different depths of one or more boreholes. In contrast, for hydraulic conductivity values, as the measured data may be scattered, the intervals associated can be defined by means of convex hulls (see Faes and Moens, 2017). This enables one to define the upper and lower bounds for hydraulic conductivity at each control point, as well as allows for assessing their dependence (Faes and Moens, 2020). These intervals can be extended to the entire domain by means of basis functions of Eq. (5), as previously analyzed.

3.3. Fuzzy approaches

3.3.1. Fuzzy variables

Another possible way of quantifying the uncertainty associated with specific parameters corresponds to applying techniques of fuzzy analysis (Beer et al., 2013a). Zadeh (1965) formally introduced this theory, which arises from necessity to represent mathematically those cases in which the knowledge of a given phenomenon is not precise, and, therefore, cannot be answered by means of classical set theory (Moens and Vandepitte, 2005; Sofi and Romeo,

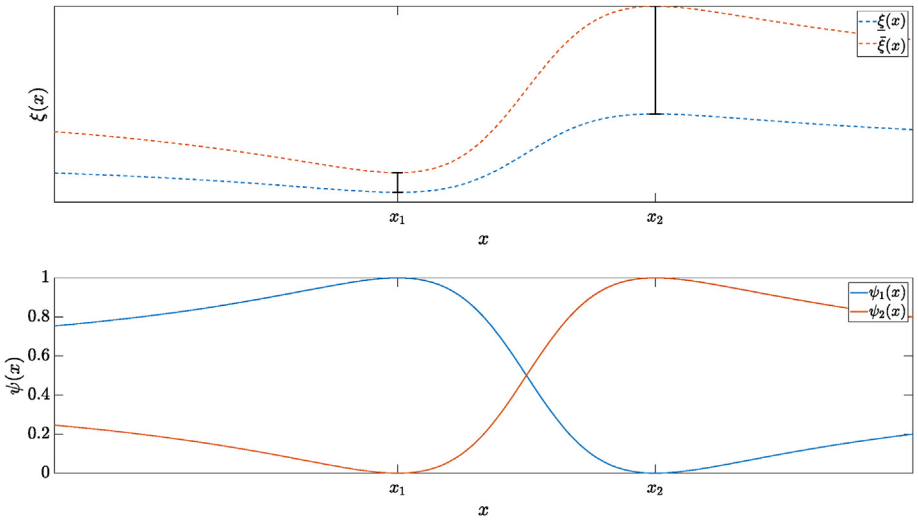

Fig. 1. Illustration of interval field with two control points (top), and basis functions associated with interval field (bottom).

2016).

In fuzzy set theory, an uncertain parameter ξ is characterized as a fuzzy variable $\widehat{\xi}$. In this context, a fuzzy variable can be interpreted as a collection of intervals, where these intervals are indexed by a membership function $\mu_{\widehat{\xi}}(\xi) \in [0,1]$. The latter holds true whenever the membership function is convex. In other words, for each of these membership levels α, there will be an interval associated with the uncertain variable ξ, i.e.

$$\xi_\alpha^I = \{\xi \in \Xi : \mu_{\widehat{\xi}}(\xi) \geq \alpha\}, \ \alpha \in (0,1] \tag{7}$$

where ξ_α^I represents the possible set of values that ξ can assume for an α-level of the membership function, and Ξ is the set that contains all physical values that ξ can accept. Note that this level corresponds to an interval whose lower and upper limits are $\underline{\xi}_\alpha$ and $\overline{\xi}_\alpha$, respectively. To illustrate the fuzzy variable concept, Fig. 2 shows the intervals associated with two specifics α-levels (α_1 and α_2 in the figure) of the membership function $\mu_{\widehat{\xi}}(\xi)$. One observes that for this case, the size of these sets of possible values decreases as the cuts are made for a membership level close to 1. This behavior is due to a triangular-shaped membership function adopted in the figure.

The membership function $\mu_{\widehat{\xi}}(\xi)$ can adopt several forms, such as triangular, trapezoidal, and sigmoidal functions, among others (Hanss, 2005). Triangular membership functions are defined by a lower bound, an upper bound, and a value associated with membership equal to one. In contrast, trapezoidal functions have an interval (i.e. collection of values) associated with the membership level one. Sigmoidal membership functions are S-shaped and have

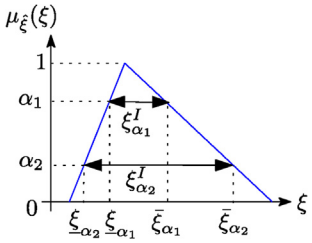

Fig. 2. Interval $\xi_{\alpha_1}^I$ and $\xi_{\alpha_2}^I$ associated with fuzzy variable $\widehat{\xi}$ for membership level α_1 and α_2, respectively.

two parameters to define them, one to control the width and one to control the center of the transition area. In this work, triangular-shaped membership functions are considered to represent the uncertainty in hydraulic conductivity. The primary purpose of its use is as a means of incorporating the sensitivity into the analysis of the interval defined at $\mu_{\widehat{\xi}}(\xi) \to 0$, by effectively propagating a set of nested intervals. This allows one to qualitatively and quantitatively investigate how the magnitude of the input uncertainty affects the response of interest. Note that this analysis assumes that the interval at $\mu_{\widehat{\xi}}(\xi) = 0$ is conservative, or at least an interval that contains as much of the available information within the limited data set as possible (Imholz et al., 2020). This type of membership function $\mu_{\widehat{\xi}}(\xi)$ is characterized by its simplicity in the construction step and efficiency during the modeling process. Specifically, note that these membership functions require scarce information for their construction (i.e. the vertex data). This information can be obtained based on expert knowledge, data available in the literature, or by means of test results, i.e. from field measurements. In the specific scenario of field measurements, the data obtained can be collected in the interval Ξ, whose lower and upper bounds correspond to the minimum and maximum measured values, respectively. Then, the crisp value to construct the fuzzy variable can be defined, for example, as the midpoint of the interval. On the other hand, data can also be visualized using histograms, which provide a preliminary notion of the shape of the membership function (Möller and Beer, 2004).

Therefore, the membership function construction is subjective and should be understood as a tool to determine how much this subjectivity affects the response of the system. One can observe that this choice does not affect the generality of the developments since in essence any convex membership function can be included in the analysis. The application of membership functions for hydraulic conductivity characterization can be also understood as a way to perform sensitivity analysis. This is because it allows different cases to be analyzed, where these cases correspond to different intervals that are indexed by the α-level under analysis. This provides additional information on the effect of, for example, hydraulic conductivity on seepage responses; yielding feedback to the users on the effect of the selected characterization of the uncertain parameters (Beer et al., 2013a).

3.3.2. Fuzzy fields

The characterization of input parameters by means of fuzzy variables, such as those described above, assumes that parameters under study are only affected by uncertainty. Nevertheless, for some variables, such as hydraulic conductivity, uncertainty is also dependent on spatial coordinates. Therefore, in the presence of spatial dependencies, the fuzzy variable concept (described in Section 3.3.1) can be extended as a fuzzy field $\widehat{\xi}(\boldsymbol{x})$. For this purpose, the interval field definition described in Section 3.2.2 can be applied. Subsequently, the key step is to define, at each control point, the membership function to capture the uncertainty in hydraulic conductivity, instead of defining intervals.

Consider the case presented in Fig. 3, where an input variable ξ exhibits spatial dependence and is characterized by the fuzzy field $\widehat{\xi}(\boldsymbol{x})$. This represents the case where there is a spatial dependence on a single coordinate. Nevertheless, the approach can be readily extended to higher dimensional problems. In the case in Fig. 3, for simplicity, there is information (i.e. physical measurements) of the input parameter at two specific locations in the domain Ω (x_1 and x_2 in Fig. 3). These locations correspond to the aforementioned control points. At each control point, it is possible to characterize the parameter as a fuzzy variable (blue membership functions in Fig. 3). For a specific membership level α, note that it is possible to associate an interval as in Eq. (7), but now at each location. These intervals correspond to $\xi^I_{1,\alpha}$ and $\xi^I_{2,\alpha}$ in Fig. 3, and they represent the possible set of values (at positions x_1 and x_2, respectively) that ξ can assume for a membership value α. Note that for this α-level, the fuzzy field $\widehat{\xi}(\boldsymbol{x})$ can be reduced to an interval field. The resulting interval field is denoted by $\xi^I_\alpha(\boldsymbol{x})$, and it corresponds to

$$\xi^I_\alpha(\boldsymbol{x}) = \sum_{j=1}^{n_b} \psi_j(\boldsymbol{x}, \boldsymbol{X}) \xi^I_{j,\alpha} \tag{8}$$

where $\xi^I_\alpha(\boldsymbol{x})$ is the interval field associated with the fuzzy variable $\widehat{\xi}$ at the location $\boldsymbol{x}$ for the membership level α, and $\xi^I_{j,\alpha}$ represents the interval at the j-th control point for a membership value α. Using basis functions ψ_j, the information at the control points is projected to any position on the domain. As a result of that procedure, the interval field associated with the α-level is obtained (red area in Fig. 3). Also, note that Fig. 3 corresponds to an extension of the top of Fig. 1, by including the membership level. It is important to emphasize that the objective of extending the interval fields to fuzzy fields is to integrate the sensitivity of the analysis to the values of the uncertain parameters defined at the control points. To achieve this, it is proposed to use triangular membership functions to construct the fuzzy field (see Fig. 3), since it allows to explore the effect of relaxing the bounds of these intervals, by linear perturbation of the input interval. Therefore, this paper does not explore the effects of using other types of membership functions.

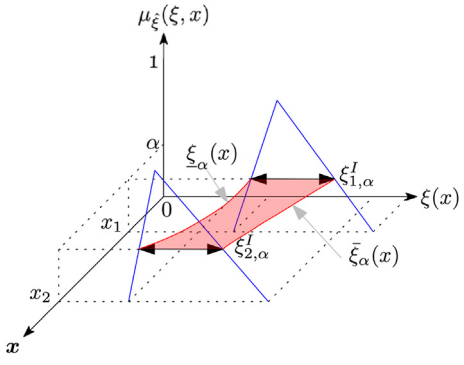

Fig. 3. Schematic representation of fuzzy field.

The interval field and fuzzy field approaches provide a framework for characterizing the uncertainty associated with a quantity $\xi(\boldsymbol{x})$, at any location in the domain Ω under study. When an uncertain property is represented by a fuzzy field, it is necessary to determine how this property is discretely represented at the level of the individual finite elements to apply the FEM. One way to perform this discretization corresponds to applying the mid-point method (Der Kiureghian and Ke, 1988), which consists of assuming that such properties, within a given finite element, can be completely described by their value at the centroid of that finite element, whose coordinate is denoted by $\boldsymbol{x}_{C,q}$, with $q = 1, \ldots, n_e$ and n_e is the number of elements. Then, the information of the uncertain parameters at the control points is propagated for each α-level, for example, to a specific centroid $\boldsymbol{x}_{C,q}$ by means of

$$\xi_{C,q} = \sum_{j=1}^{n_b} \psi_j(\boldsymbol{x}_{C,q}, \boldsymbol{X}) \xi_j, \ \xi_j \in \xi^I_{j,\alpha} \tag{9}$$

where $\xi_{C,q}$ corresponds to the value of the uncertain parameter at the centroid of the element q, and $\psi_j(\boldsymbol{x}_{C,q}, \boldsymbol{X})$ are the basis functions evaluated at the centroid coordinates of the q-th finite element.

Fig. 4 shows an illustration of the construction of the fuzzy field from measured data. Similar to the construction of interval fields (see Section 3.2.2), which requires retrieving hydraulic conductivity data (for seepage analysis) at control points, the first step in constructing the fuzzy field from site-specific observations is to define the hydraulic conductivity at those locations. This is illustrated in Fig. 4a when measurements are collected at two locations in the domain. The hydraulic conductivity data used in Fig. 4 can be found in the work of Arshad et al. (2020). Note that given these field data, the boundaries of the intervals representing hydraulic conductivity at both locations can be identified, as shown in Fig. 4b, and the resulting interval field can be calculated according to Eq. (8). Also note that since this is a simplified example in terms of dimensionality and number of uncertain parameters, one way to define these intervals is to consider the minimum and maximum values of the soil property at these positions. Nevertheless, for more complex systems, the corresponding intervals can be defined using convex hulls (see Faes and Moens, 2017), or using a Bayesian approach, which allows one to assess the reliability of the bounds (see Imholz et al., 2020). Since the defined bounds are very sensitive to outliers in the dataset, it is necessary to know how sensitive the response is to perturbations of the intervals. Hence, the associated intervals from the interval field framework can be extended to triangular membership functions when using fuzzy fields, as shown in Fig. 4c. The triangular membership functions (defined with the aim to perform a sensitivity analysis) define the mid-point of the intervals with membership equal to one. Note how the interval field associated with the membership level approaching 0 (in green in Fig. 4d) becomes narrower as the membership level being analyzed approaches one (see interval fields in yellow). This discrete representation of the fuzzy field allows one to perform seepage analysis considering the uncertainty of the hydraulic conductivity.

3.4. Uncertainty propagation

The previous subsections discussed techniques to incorporate hydraulic conductivity uncertainty into a finite element model for performing a seepage analysis. After describing the uncertainty in hydraulic conductivity, it is necessary to propagate this uncertainty to the response by considering spatial dependencies. When the

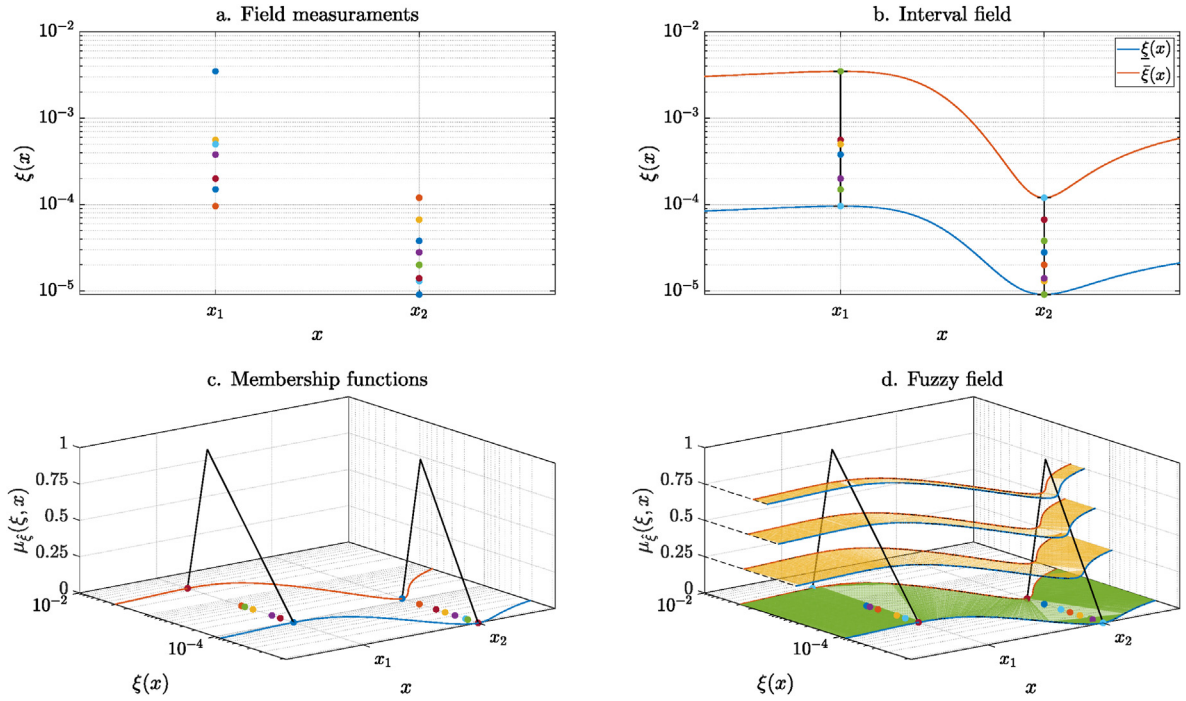

Fig. 4. Procedures for constructing the fuzzy field.

input parameters are characterized as fuzzy parameters, the response depends on the analyzed membership level, which means that the response of the system r is also a fuzzy variable $\hat{r}$. Several methods are available to perform fuzzy analysis, such as the transformation method, developed by Hanss (2005) to propagate the fuzzy uncertainty through a numerical model; and the α-level optimization (Möller et al., 2000). Following the latter methodology, the membership function associated with the response of a system $\mu_{\hat{r}}(r)$ is calculated according to the interpretation of a fuzzy variable given in Section 3.3.1. For this purpose, the membership function at each control point $\mu_{\hat{\xi}_j}(\xi_j)$ is analyzed for discrete membership values α_l, with $l = 1, \ldots, n_c$, where n_c indicates the number of discrete levels considered. That is, for a given membership level α_l, the response of interest r will be contained in an interval r_α^l with lower $\underline{r}_{\alpha_l}$ and upper $\bar{r}_{\alpha_l}$ bounds. In mathematical terms, we have

$$\underline{r}_{\alpha_l} = \min_{\xi_j} \left[r(\xi_1, \xi_2, \ldots, \xi_{n_b}) \right], \ \xi_j \in \xi_{j,\alpha_l}^I, \ j = 1, \ldots, n_b, \ \ l = 1, \ldots, n_c \tag{10}$$

$$\bar{r}_{\alpha_l} = \max_{\xi_j} \left[r(\xi_1, \xi_2, \ldots, \xi_{n_b}) \right], \ \xi_j \in \xi_{j,\alpha_l}^I, \ j = 1, \ldots, n_b, \ l = 1, \ldots, n_c \tag{11}$$

where $\xi_1, \xi_2, \ldots, \xi_{n_b}$ denotes the value of the uncertain property at the j-th control point associated with the membership level α_l. Thus, after the optimization procedure, the extreme values of the response of interest (e.g. total flow, uplift force, and exit gradient) are computed for the membership level under analysis. The α-level optimization procedure is schematized in Fig. 5. Consider that hydraulic conductivity has been characterized at two positions in the domain Ω by means of the membership functions $\mu_{\hat{\xi}_1}(\xi_1)$ and $\mu_{\hat{\xi}_2}(\xi_2)$ as was discussed in Section 3.3.2. To estimate the membership function of the response r, two α-levels were considered. For each of these levels, the intervals associated with hydraulic conductivity at each location in Ω are retrieved. Then, for both α_1 and α_2 levels, an interval analysis is performed to estimate the bounds of the response by solving Eqs. (10) and (11). Note that to find the response value for a membership level equal to 1, a deterministic analysis must be performed, since for this membership level there is no associated interval to the uncertain parameters. The aforementioned is valid due to the assumption of using triangular membership functions. As a result, a discrete representation of the membership function of the response $\mu_{\hat{r}}(r)$ can be obtained for the two membership levels α_1 and α_2 under consideration.

In this contribution, the response of interest r can correspond to the seepage total flow, uplift force, or exit gradient. For example, if the focus is on total flow as the response of interest, then solving Eqs. (10) and (11) yields the interval estimates (for each membership level) that provide insight into the degree of uncertainty given the input uncertain hydraulic conductivity. Note that Eqs. (10) and (11) are functions of ξ_j ($j = 1, \ldots, n_b$). Hence, once the hydraulic conductivity is characterized by means of membership functions at the control points, the uncertainty in the problem is reduced to that present at these locations. Therefore, the aim is to propagate the uncertainty present at the control points to the response of interest r, for each membership level. The lower $\underline{r}_{\alpha_l}$ and upper $\bar{r}_{\alpha_l}$ bounds of the response from Eqs. (10) and (11), respectively, are determined by optimization. In this work, to compute the membership levels taken into account, the Particle Swarm optimization scheme (Kennedy and Eberhart, 1995) is applied.

Once the uncertainty has been propagated, analysts can gain an idea of the degree of variation in the seepage responses, as well as feedback from the definition of the input parameters. Since obtaining additional field measurements can be costly and time-consuming, validating the membership functions used to construct the fuzzy field by analyzing the response membership

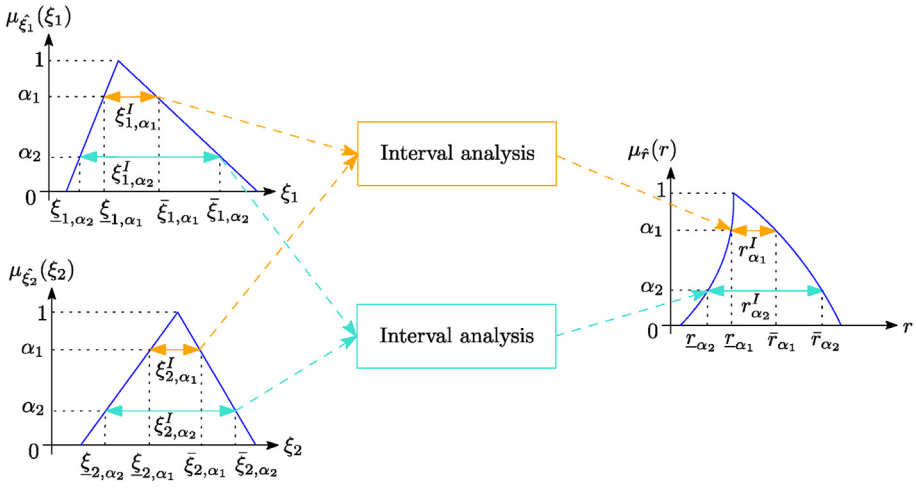

Fig. 5. Graphical representation of the α-level optimization procedure, applied to two fuzzy variables $\hat{\xi}_1$ and $\hat{\xi}_2$ to obtain the response $\hat{r}$.

functions is a practical approach. For example, if the membership functions describing the seepage responses show minimal variation, it raises the question of whether the definition of the input parameters adequately accounts for the uncertainty. Thus, analysis of the membership functions of the response can be a useful tool for validation, indicating the adequacy of the fuzzy field representation for capturing and propagating uncertainty in the system.

3.5. Summary of the proposed strategy

The strategy for performing fuzzy seepage analysis considering that hydraulic conductivity is represented by a fuzzy field can be summarized in the following steps, which are also illustrated in Fig. 6:

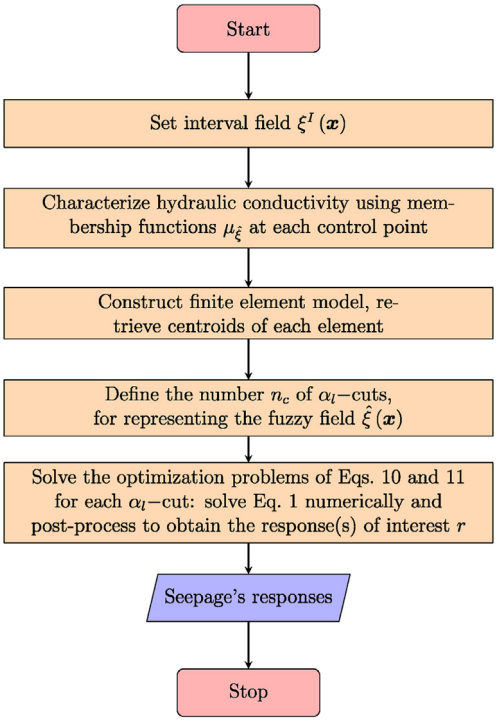

Fig. 6. Flowchart of the seepage analysis with fuzzy fields.

(1) Set the interval field according to available data, as explained in Section 3.2.2.
(2) Set the membership functions at the control points, as shown in Section 3.3.1.
(3) Define the finite element model. For each element, retrieve its centroid.
(4) Define the number of membership levels to be considered for discretely representing the fuzzy field.
(5) For each level, solve the optimization problems of Eq. (10) (for the lower bound) and (11) (for the upper bound) to obtain the response of interest r. The specific steps are:
  (i) Map the uncertainty from the control points to the finite element centroids using Eq. (9).
  (ii) Solve the governing equation (Eq. (1)) numerically, considering the uncertainty, i.e. evaluate Eq. (3) for the values defined in step (i).
  (iii) Post-process the result obtained from Eq. (3) to determine the bounds of the response of interest.

4. Analysis and results

4.1. Illustrative example

The analysis of steady-state confined seepage below an impermeable dam containing two cut-off walls is considered to illustrate the proposed approach. The geometric definition of the system has been defined for illustrative purposes and is shown in Fig. 7. The numerical model was based on different studies in the literature (Griffiths and Fenton, 1993; Hekmatzadeh et al., 2018; Valdebenito et al., 2019). The dam is founded on a permeable soil layer of 20 m depth, limited by an impermeable rock layer. The upstream side of the dam retains a water column with a deterministic height of 10 m. Upstream flow occurs where the hydraulic head is 10 m and downstream flow occurs where the hydraulic head is 0 m. From left to right, the cut-off walls are 4 m and 10 m long (see Fig. 7). The flow is assumed to be zero at the boundaries of the cut-off walls and along the bottom, left, and right edges of the permeable soil layer. The objective is to determine the flow that drains downstream of the dam, the uplift force at the base of the dam, and the exit gradient.

The horizontal k_H and vertical k_V hydraulic conductivities are characterized as fuzzy fields. Four control points were considered to emphasize the effectiveness of the approach when few measurements are available. Note that in previous studies, a sample size

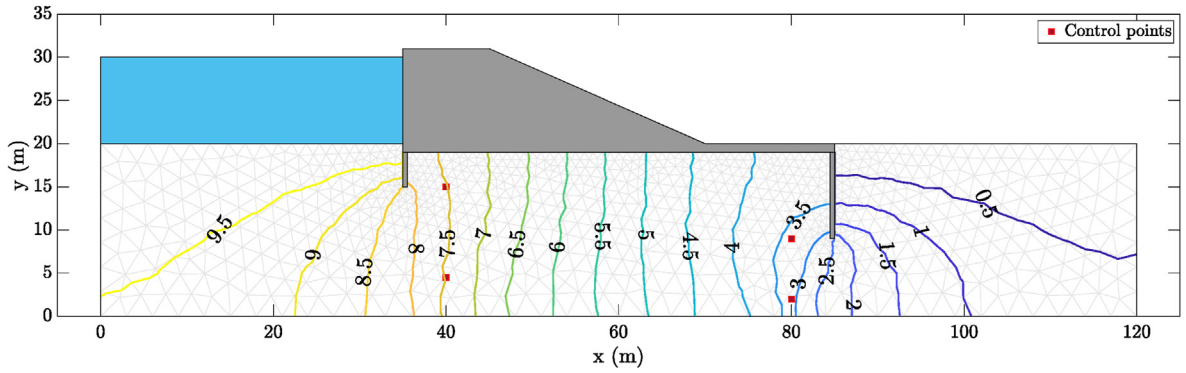

Fig. 7. Finite element mesh and control point locations. The contour lines represent the piezometric head h results for the hydraulic conductivity values associated with a membership level $\mu_{\hat{k}}(k) = 1$.

of less than 7 for a geotechnical context is considered a strong indicator for the use of intervals (Beer et al., 2013b). Therefore, a fuzzy field approach, which allows one to consider the sensitivity of the intervals defined at the control points, seems reasonable to incorporate the uncertainty in hydraulic conductivity into the seepage analysis, indicating an awareness of the potential limitations of using a small number of observations. Hence, it is assumed that field measurements allow modeling the horizontal hydraulic conductivity through fuzzy sets, as discussed in Section 3.3.2. The membership function at each control point for horizontal hydraulic conductivity is shown in Fig. 8. Note that these membership functions were constructed with the vertex data (see Table 1), where the values associated with a membership level of one were considered the mid-point of the intervals. As discussed in Section 3.3.1, this data can be obtained from expert knowledge, existing evidence in the literature, or by conducting field measurements. In this work, the values for horizontal hydraulic conductivity have been defined according to field measurements of literature reports (Elhakim, 2016) for illustrative purposes. On the other hand, vertical hydraulic conductivity values are characterized considering the following relationship: $0.1k_H \leq k_V \leq k_H$, which allows one to account for the dependence between both horizontal and vertical

Table 1
Interval data at control points for horizontal hydraulic conductivity k_H. Vertical hydraulic conductivity k_V values are characterized considering the following relationship: $0.1k_H \leq k_V \leq k_H$.

Control point	Position (m)	k_H (m/s)
Control point 1	$x = 40, y = 15$	$[2 \times 10^{-6}, 5.6 \times 10^{-5}]$
Control point 2	$x = 40, y = 4.5$	$[4 \times 10^{-7}, 1.44 \times 10^{-5}]$
Control point 3	$x = 80, y = 9$	$[2 \times 10^{-6}, 8.2 \times 10^{-5}]$
Control point 4	$x = 80, y = 2$	$[7 \times 10^{-8}, 1.57 \times 10^{-6}]$

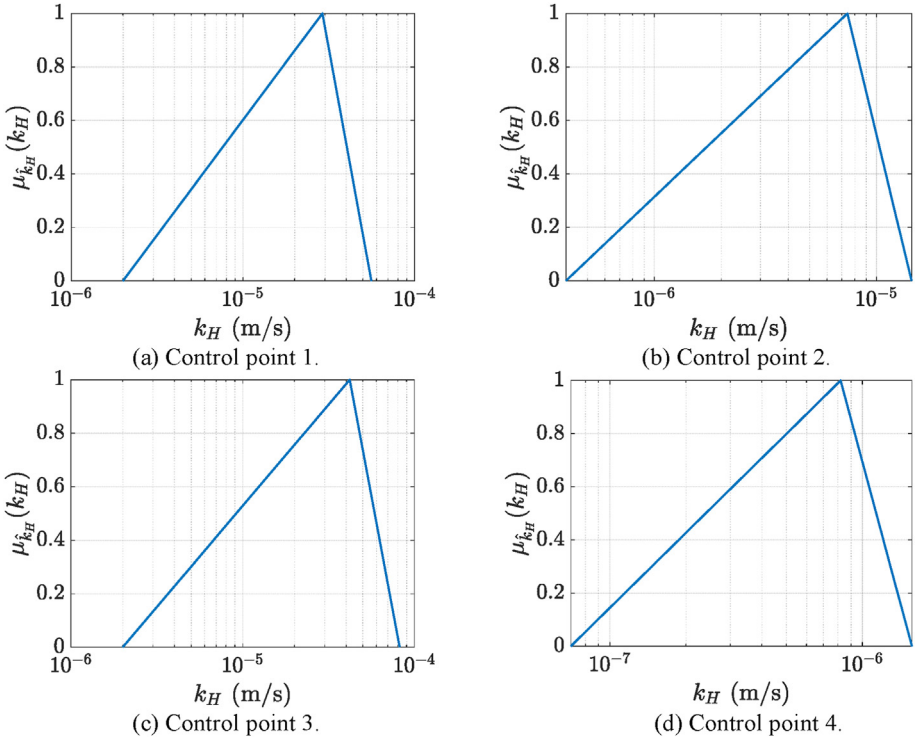

Fig. 8. Membership function of horizontal hydraulic conductivity at control points. The control points are located at (a) $x = 40$ m , $y = 15$ m; (b) $x = 40$ m , $y = 4.5$ m; (c) $x = 80$ m , $y = 9$ m; and (d) $x = 80$ m , $y = 2$ m.

hydraulic conductivities, as well as to incorporate the physical anisotropy of the conductivities. The preceding relation between horizontal and vertical hydraulic conductivity is based on typical values available in the literature. The lower bound is selected on the basis that normally vertical hydraulic conductivity is about one-tenth of the horizontal hydraulic conductivity (Fanchi, 2010). The upper bound is defined considering that both hydraulic conductivities can become equal (Shedid, 2019).

It is noteworthy that since the problem is 2D and physically anisotropic, it is not possible to visualize the resulting fuzzy field, as shown in Fig. 3. The reason is that the resulting fuzzy field has two dimensions related to each hydraulic conductivity (k_H and k_V), another two dimensions related to each spatial dimension of the domain, and the dimension corresponding to the degree of membership. However, Fig. 9 shows the membership functions defined for each control point. It is observed that these figures are an extension of the membership functions shown in Fig. 8, considering both horizontal and vertical conductivities. These membership functions correspond to irregular pyramids. The trapezoidal shape of the base of the membership functions (i.e. when $\mu_{\hat{k}}(k) = 0$) is due to (1) the considered relationship between the vertical k_V and horizontal k_H hydraulic conductivities; and (2) the physical anisotropy of the hydraulic conductivity. Note how, owing to the logarithmic scale of the axes, the base of the pyramids looks like a rhomboid. Note that the considered dependence between both conductivities yields physically sound values for characterizing hydraulic conductivity.

Note also that for a given membership level, it is possible to visualize the horizontal and vertical hydraulic conductivity fields separately. Fig. 10 shows three realizations of both hydraulic conductivities from the base of the pyramids of Fig. 9 (i.e. when $\mu_{\hat{k}}(k) = 0$). This figure shows the change in the resulting field due to variations in the hydraulic conductivity values at the control points. The differences between the resulting field for horizontal and vertical hydraulic conductivities are also observed due to the anisotropy considered in the soil property. Note how certain realizations result in fields with less spatial variation in the hydraulic conductivity. As a result, the hydraulic conductivity of the soil layer tends to be closer to the average of the values associated with the control points. Conversely, some realizations show more pronounced local effects of the conductivity values at the control points, resulting in a field with more spatial variation. It is also generally observed that vertical hydraulic conductivity values tend to be lower than horizontal values.

A convergence study was performed to determine the layout of the finite element mesh. For this purpose, it was verified that there were no significant variations in the interval of response obtained for a specific membership level. The finite element model selected comprises 3821 nodes and 1822 quadratic triangular elements. A total of 10 α-levels have been used to estimate the response membership function, i.e. $n_c = 10$. The hydraulic conductivity matrix of each element was calculated using numerical integration, considering 3 integration points. It is important to highlight that due to the characterization of the parameters described previously,

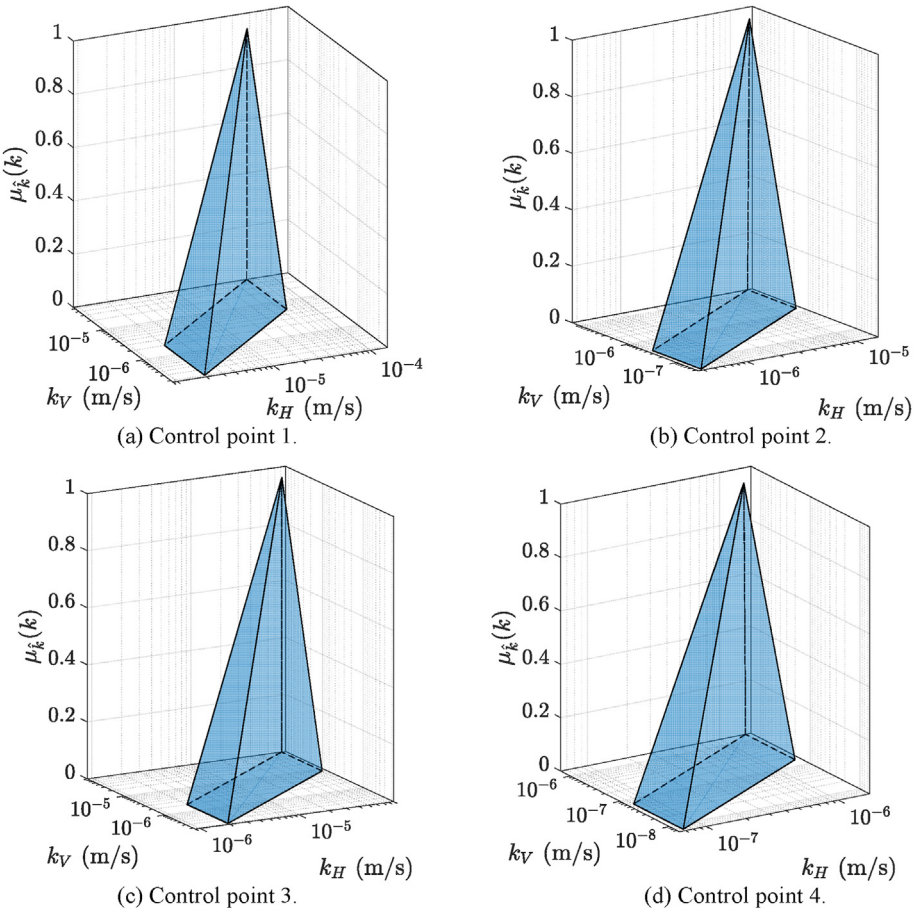

Fig. 9. Membership function of hydraulic conductivity at control points. The control points are located at (a) $x = 40$ m , $y = 15$ m; (b) $x = 40$ m , $y = 4.5$ m; (c) $x = 80$ m , $y = 9$ m; and (d) $x = 80$ m , $y = 2$ m.

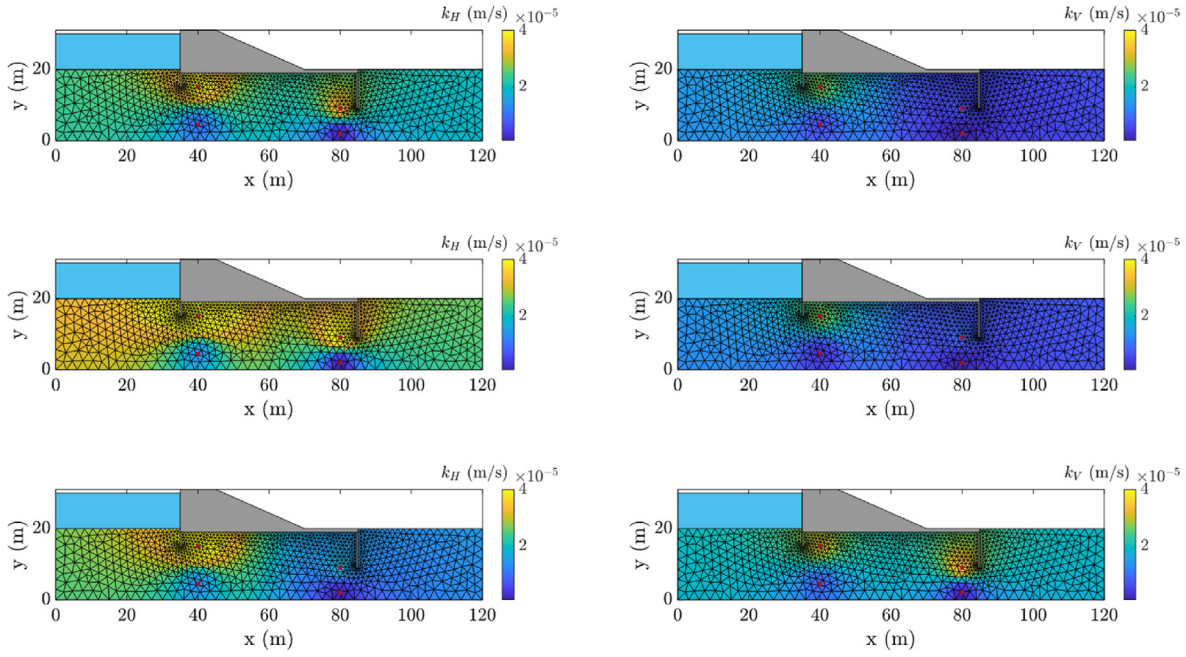

Fig. 10. Fuzzy field realizations for horizontal and vertical hydraulic conductivities for membership level approaching zero: Horizontal conductivity (left), and Vertical conductivity (right).

the flow rate, uplift force, and exit gradient are also uncertain. When non-probabilistic methods are used, traditional statistical measures such as mean, standard deviation, and coefficient of variation cannot be used to describe the system's response. On the contrary, when fuzzy approaches are used to characterize uncertain parameters, the response is fuzzy as well and is obtained in the form of membership functions. Therefore, the objective of this study will be to determine the membership function that represents the uncertainty in the flow rate, uplift force, and exit gradient. To estimate the membership levels considered for each response, the particle swarm optimization scheme (Kennedy and Eberhart, 1995) was applied.

4.2. Total flow

The total flow discharge of the dam is a key result of the seepage analysis and is of utmost importance for design purposes. Accurate estimation of the total flow discharge is essential for sizing drainage systems, determining the potential for erosion or piping, and evaluating the overall stability of the structure (Hekmatzadeh et al., 2018). The seepage flow rate is calculated in terms of the unit width of the dam, after determining the piezometric height (Valdebenito et al., 2019). For this purpose, the summation of the flow over all boundary nodes on the left side of the dam was computed to yield the total flow (Degrauwe et al., 2010). The membership function obtained for the total flow response is shown in Fig. 11. The values in the figure correspond to the total flow r_q normalized by the value obtained for the deterministic analysis r_{q_0} at $\mu_{\hat{r}_q}(r_q) = 1$. Therefore, the flow response is denoted as r_q/r_{q_0} in Fig. 11. The total flow at the membership level equal to 1 r_{q_0} is 3.87×10^{-5} m^3/s per m. This analysis represents a deterministic evaluation of the system, which considered the values of the hydraulic conductivities at the control points associated with a membership equal to one.

As explained earlier in this work, as hydraulic conductivity is characterized by means of fuzzy fields, then the response in terms of the total flow becomes fuzzy as well. Hence, the flow response must be interpreted according to the membership level analyzed,

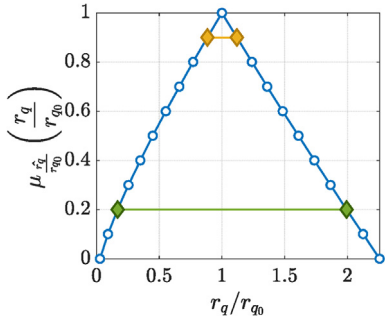

Fig. 11. Membership function associated with total flow response. Values normalized by the total flow equal to 3.87×10^{-5} m^3/s per m for $\mu_{\hat{r}_q}(r_q) = 1$. The responses associated with levels $\alpha = 0.9$ and $\alpha = 0.2$ are highlighted in yellow and green, respectively.

which provides insights into the degree of uncertainty associated with the flow response. For example, for the membership level of 0.9 highlighted in yellow in Fig. 11, the total flow is between 0.88 and 1.12 times the value for membership level 1. Whereas, for the membership level 0.2, highlighted in green in Fig. 11, the total flow can take any value between 0.17 and 1.99 times the deterministic value. The observed variation between the limits of the two intervals mentioned above is explained by the influence of hydraulic conductivity. Since k_H and k_V are considered uncertain, this uncertainty propagates to the flow response, leading to different cases to analyze. With this information, users can have feedback on the effect of the selected characterization of the uncertain parameters, improving the understanding and trustworthiness of the analysis. Hence, the resulting membership function should be regarded as a means of analyzing the sensitivity of the bounds of the response. Furthermore, analyzing the shape of the membership function obtained for the total flow provides additional valuable information. From the shape of the membership function in Fig. 11, a nearly linear relationship between the membership level under analysis and the flow response was obtained.

4.3. Uplift force

The seeping water causes a hydraulic gradient between the upstream and downstream sides of the dam. This hydraulic gradient induces a vertical upward pressure. This upward pressure is known as the uplift force (Terzaghi and Peck, 1967). Uplift pressures can lead to instability and potential failure if not properly addressed (Mansuri et al., 2014). Thus, uplift is an active force that should be incorporated into the stability analysis (Norouzi et al., 2020). In this work, the uplift force at the base of the dam was calculated by integrating the piezometric head distribution at the base of the dam. This process was carried out by means of the trapezoidal numerical integration scheme.

The membership function obtained for the uplift force response is shown in Fig. 12. The figure shows the values of the uplift force r_u normalized by the value associated with a membership level equal to 1 r_{u_0}. The uplift force for a membership level equal to 1 is 273.14 t/m, which corresponds to a deterministic analysis. A linear relationship between the membership level under analysis and the uplift force is noted by the shape of the membership function of Fig. 12. For practical purposes, the maximum possible value of the uplift force should be considered for the stability analysis (Mansuri et al., 2014; Hekmatzadeh et al., 2018). The reason behind this is that high uplift force reduces the effective normal stress and, as a result, decreases the frictional resistance, causing the structure to be more susceptible to sliding failure (Terzaghi and Peck, 1967). For the particular case in Fig. 12, the variation of the maximum uplift force with respect to that associated with a membership level 1 was close to 1.7 times.

The optimization of the α-level reveals the presence of two distinct uplift force responses, representing the best scenario (minimum r_u) and the worst scenario (maximum r_u) across the ten α-levels considered to estimate the fuzzy response. These responses correspond to the extreme cases where the uncertainty in hydraulic conductivities has the greatest impact on the uplift force. By exploring these two distinct responses, the analysis captures the range of possible values of uplift force and provides valuable insights into its potential variability under different scenarios. For example, if the membership level 0.3 is studied (see yellow interval in Fig. 12), the uplift force is between 0.47 and 1.52 times the deterministic value. Whereas, for the membership level approaching 0 (see green interval in Fig. 12), the uplift force can take any value between 0.24 and 1.74 times the deterministic value. This variation, between the boundaries of the two intervals, was less than the one observed with the flow response. Such behavior is explained because the uplift response is strongly influenced by the value of the water height retained upstream of the dam, which was considered deterministic.

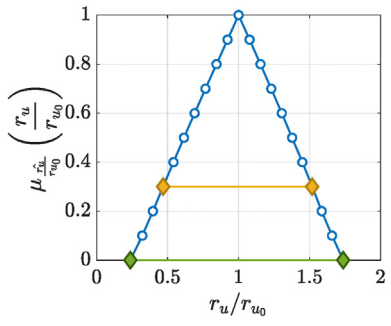

Fig. 12. Membership function associated with uplift force response. Values normalized by the uplift force equal to 273.14 t/m for $\mu_{\hat{r}_u}(r_u) = 1$. The responses associated with levels $\alpha = 0.3$ and $\alpha = 0$ are highlighted in yellow and green, respectively.

The application of a fuzzy approach in this study also enables one to understand the behavior of the seepage flow for the critical cases identified in the uplift force analysis. Fig. 13 shows the variation of the piezometric heights of levels 1, 3, 6, and 9 m obtained for the solution associated with a membership level equal to one (Case A in the figure), with respect to the solution considering the hydraulic conductivities associated with the lower bound (Case B) and upper bound (Case C) of the uplift force response at an α-level approaching 0. For Case B, the contour lines appear shifted to the left with respect to the nominal solution for $\mu_{\hat{k}}(k)$. The minimum uplift force response was associated with smaller hydraulic conductivities at the control points on the left compared to the right (see Fig. 14). This leads to slower flow and, therefore, lower pressures at the base of the dam. In contrast, for Case C, the curves shift considerably to the right compared to the nominal solution for $\mu_{\hat{k}}(k) = 1$ (see Fig. 14), resulting in increased pressures below the dam. These results are attributed to higher values of hydraulic conductivities on the control points to the left compared to the right, leading to faster water flow. The examination of such cases provides a more comprehensive view of the behavior of the seepage flow. For instance, this analysis permits to detect drainage or water retention problems (Hager et al., 2020).

4.4. Exit gradient

The exit gradient corresponds to the rate of change of the piezometric head at the exit point closest to the dam at the downstream end (Griffiths and Fenton, 1993). For exit gradient recovery, the first derivative of the piezometric head at superconvergent points (Zienkiewicz, 2000) was calculated. In this work, these points corresponded to the Gauss points of the reduced integration scheme (Previati et al., 2019; Ding et al., 2021). The exit gradient obtained after the seepage analysis is usually compared to the critical gradient i_c. Revising the exit gradient is of utmost importance since a value higher than the critical gradient would initiate piping (Griffiths and Fenton, 1998; Liu et al., 2017b). This phenomenon refers to the movement of soil particles carried away by the percolating water, creating underground pathways or tunnels (Mansuri et al., 2014). It is usually accepted that the critical hydraulic gradient is approximately equal to 1 for vertical flow conditions in deterministic analyses (Terzaghi and Peck, 1967), however, some evidence shows that i_c can range from 0.88 to 1.27 (Meyer et al., 1994).

The membership function obtained for the exit gradient response is shown in Fig. 15. The figure shows the values of the exit gradient r_i normalized by the value associated with a membership level equal to 1 r_{i_0}. Due to the shape of the membership function, a nonlinear relationship between hydraulic conductivity and the exit gradient was observed. The exit gradient for $\mu_{\hat{r}_i}(r_i) = 1$ corresponds to 0.14, which is less than the value of the critical gradient $i_c = 1$. In comparison with the total flow and uplift force analyzed, a bit wider variation with respect to the value associated with a membership level equal to 1 was obtained for the exit gradient. Hence, this response exhibited a larger sensitivity with respect to the membership level under analysis. This higher sensitivity was obtained at the right end of the exit gradient membership function. This phenomenon is strongly significant since this portion of the membership function exhibits the maximum values of the exit gradient that may indicate the possibility of piping. Furthermore, users can analyze the evolution of the safety factor against piping according to the membership level.

As previously shown for the results in terms of total flow and uplift force, the response associated with the exit gradient must be interpreted as a result of the membership level analyzed. For

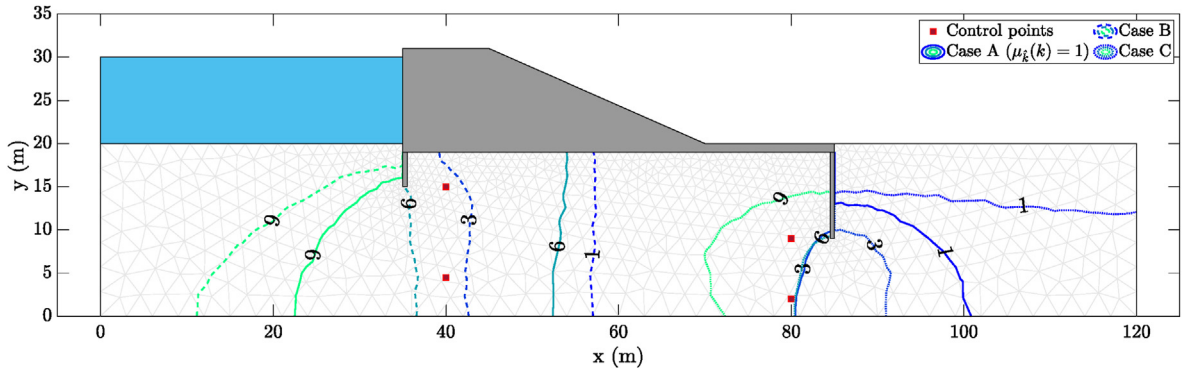

Fig. 13. Piezometric head h results for: Case A, $\mu_{\hat{k}}(k) = 1$; Case B, piezometric head h for hydraulic conductivities found for lower bound level approaching 0 uplift force; Case C, piezometric head h for hydraulic conductivities found for upper bound level approaching 0 uplift force.

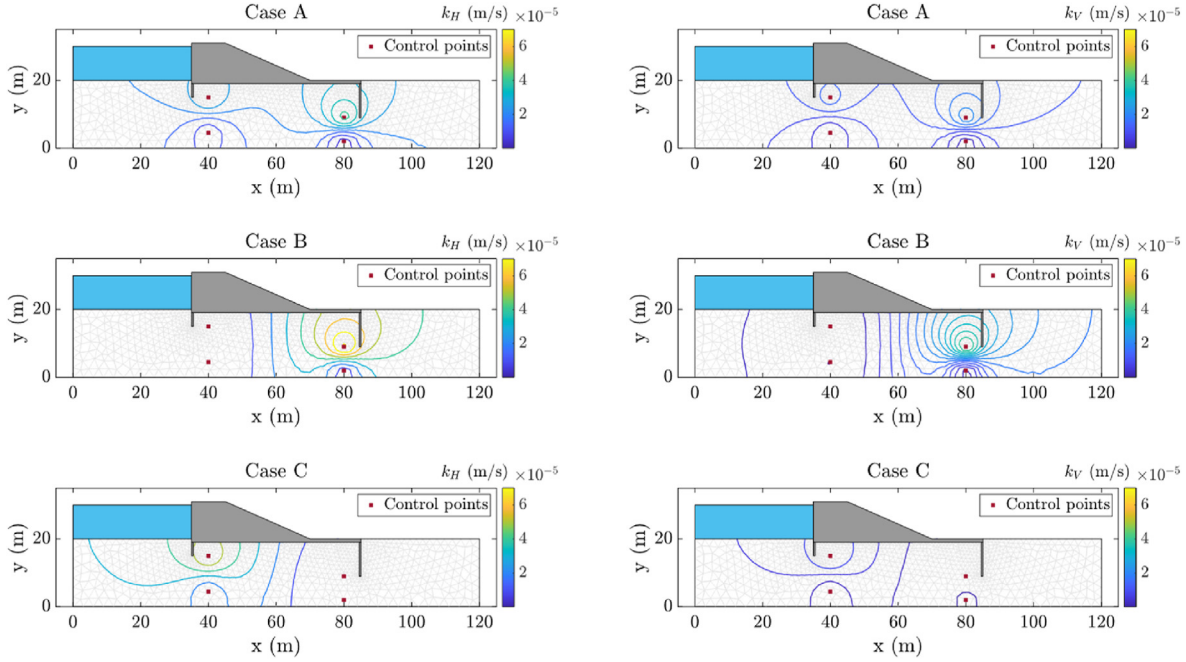

Fig. 14. Horizontal (left) and vertical (right) hydraulic conductivities for uplift force results. Case A, hydraulic conductivity fields for uplift force results at $\mu_{\hat{k}}(k) = 1$; Case B, hydraulic conductivity fields for uplift force results at lower bound level approaching 0; Case C, hydraulic conductivity fields for uplift force results at upper bound level approaching 0.

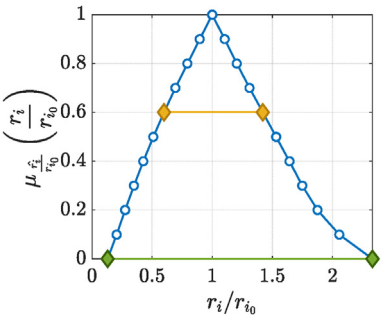

Fig. 15. Membership function associated with exit gradient response. Values normalized by the exit gradient equal to 0.14 for $\mu_{\hat{r}_i}(r_i) = 1$. The responses associated with levels $\alpha = 0.6$ and $\alpha = 0$ are highlighted in yellow and green, respectively.

example, if the membership level of 0.6 is considered (see yellow interval in Fig. 15), the exit gradient can take any value between 0.60 and 1.42 times the exit gradient at $\mu_{\hat{r}_i}(r_i) = 1$, which corresponds to the deterministic analysis. The maximum value associated with a membership level approaching 0 (see green interval in Fig. 15) is about 2.33 times more than the value obtained by the deterministic analysis, which agrees with the reported values in the literature (Griffiths and Fenton, 1993, 1998).

Similar to the analysis conducted for the variation of the seepage flow for the extreme cases of the uplift force response, the same procedure was applied while considering the results of the exit gradient for the membership level approaching 0. Fig. 16 shows the variation of the levels of piezometric heights 1, 3, 6, and 9 m with respect to the nominal solution for $\mu_{\hat{k}}(k) = 1$. For Case B, the levels 1, 3, and 6 were displaced to the left with respect to the nominal solution for $\mu_{\hat{k}}(k) = 1$, with behavior similar to that observed for the uplift force response. Nevertheless, the 9-m contour curve exhibited a smaller shift (with respect to the nominal solution) compared to that obtained for the uplift force response. On the other hand, for Case C the curves for 1, 3, and 6 m are slightly

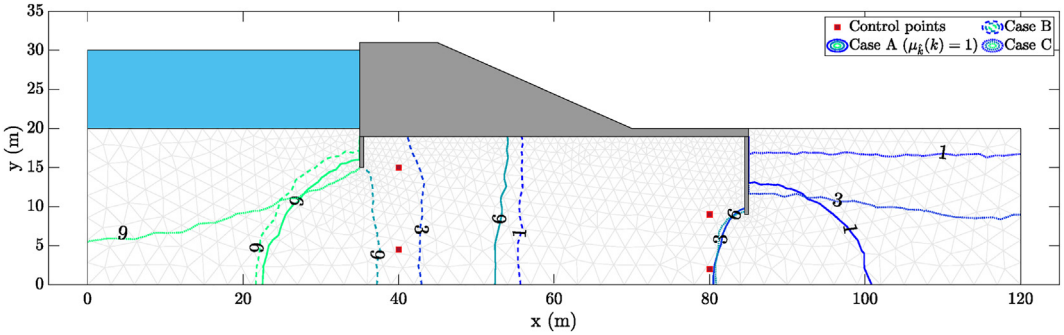

Fig. 16. Piezometric head h results for: Case A, $\mu_{\hat{k}}(k) = 1$. Case B, piezometric head h for hydraulic conductivities found for lower bound level approaching 0 of exit gradient; Case C, piezometric head h for hydraulic conductivities found for upper bound level approaching 0 of exit gradient.

displaced to the right compared to the nominal solution for $\mu_{\hat{k}}(k) = 1$, while the 9-m contour curve shifted to the right. Moreover, for Case C, the piezometric head values in the vicinity of the dam exit were higher than in the case analyzed with the uplift force response for the membership level approaching 0. The aforementioned scenario is of utmost importance since a high piezometric head at the exit of the dam necessitates proper monitoring to ensure the safe and efficient operation of the dam (Hager et al., 2020).

4.5. Sensitivity analysis

A sensitivity analysis was carried out to study the influence of parameter p of the basis functions on the membership functions of the responses. This parameter affects how the interpolation of the intervals works based on the distance to the control points. Values of $p = 1, 1.5$, and 2 have been studied. These values of p were defined according to those reported in the literature (De Mulder et al., 2012).

The membership functions obtained for the flow response, for the different cases analyzed, are shown in Fig. 17. The flow response exhibited minimal sensitivity to the variation of the parameter p. The low variation of this response for the different values of p tested can be explained because very similar ranges of hydraulic conductivities were obtained over the domain. Even though a lower value of p increases the local influence of the interval defined at control points, as the flow quantity represents an integrated, overall behavior of the system, local fluctuations in uncertainty do not affect the fuzzy response. Furthermore, for the deterministic case, i.e. for $\mu_{\hat{r}_q}(r_q) = 1$, no significant differences were observed for the different values of p analyzed.

The membership functions calculated for the uplift force response for $p = 1, 1.5,$ and 2, are shown in Fig. 18. The uplift force response shows a high sensitivity to the value of p at the left-end,

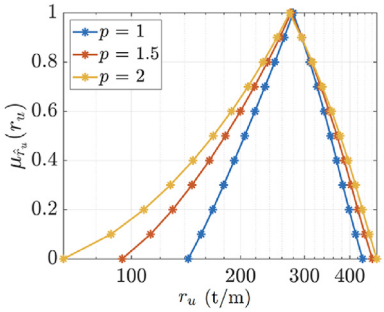

Fig. 18. Membership function associated with uplift force response for $p = 1, 1.5$ and 2.

which increases closer to $\mu_{\hat{r}_u}(r_u) = 0$. This is because this quantity is influenced by the local effects of the control points near the base of the dam. The case of $p = 2$ corresponds to the worst-case scenario for the right-hand side of the membership function. Nevertheless, for the response shown in Fig. 18, the intervals obtained for the different α-cuts for the values of $p = 1$ and 1.5, are contained in the intervals determined for $p = 2$, which is a product of local effects. Precisely, a smaller value of p yields a localisation of the uncertainty in a more compact sub-domain of the physical domain. Regarding the deterministic scenario, i.e. for $\mu_{\hat{r}_u}(r_u) = 1$, quite small differences were observed for the different values of p analyzed.

Sensitivity analysis results of the exit gradient with respect to the values of the parameter p are shown in Fig. 19. The exit gradient response shows similar behavior to the uplift force. The membership functions obtained show a high sensitivity at the left end when comparing the results for $p = 1, 1.5$, and 2. Therefore, local

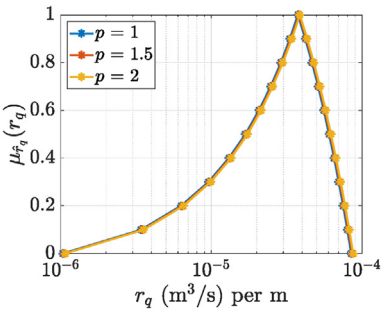

Fig. 17. Membership function associated with seepage flow response for $p = 1, 1.5$ and 2.

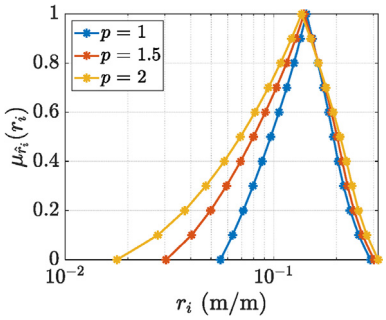

Fig. 19. Membership function associated with exit gradient response for $p = 1, 1.5$ and 2.

influences on the intervals near the control points, adjacent to the dam exit, are controlling the exit gradient fuzzy response. Moreover, the effect of the parameter p yielded a larger difference on the left side of the membership functions, where this difference became larger as the membership levels closer to 0 were analyzed. The largest values for the right end, which are relevant for design purposes, were obtained for a value of $p = 2$. Concerning the deterministic analysis, i.e. for $\mu_{\tilde{r}_i}(r_i) = 1$, small differences were observed for the different values of p.

4.5.1. Random or fuzzy fields?

The decision to propose fuzzy fields as an alternative tool for dealing with uncertainty in soil hydraulic conductivity in seepage analysis, compared to traditional stochastic approaches such as random fields, was driven by several factors in this study. These factors can be summarized as the amount of data typically available for seepage analysis, the number of assumptions to be made, and the intended purpose of the analysis. Within the same system under analysis, if the user has sufficient information to select an appropriate probability density function, autocorrelation function, and corresponding length parameter, then a random field can be used to accurately describe the uncertainty. As a result, the random field characterization will provide a comprehensive probabilistic representation of the response of interest, which can be used for reliability analysis (Liu et al., 2017a; Sharma et al., 2021). However, if only a few measurements are available and only the bounds of the uncertain parameters can be defined, then an interval or fuzzy field representation allows one to account for those measurements to describe the uncertainty and, moreover, to study the sensitivity of those bounds (Chen et al., 2020). Here, the only assumption other than the bounds on the uncertain parameters (at the positions where the data were measured) is the power p of the basis functions, which, as shown in the previous section, does not have a large impact on the critical values of the analyzed responses. The result of a characterization by means of fuzzy fields will then lead to extreme values of the response for different membership levels, which can be interpreted in terms of interval estimates with their sensitivity, providing insight into the degree of uncertainty. More recently, hybrid approaches have been developed. For example, distribution-free P-boxes provide a robust and consistent way to characterize uncertainty when data are sparse but random in nature (Faes et al., 2022). Another example is Gaussian random fields using the Karhunen-Loève (K-L) expansion with imprecise covariance kernels. This imprecise random fields have also been developed to deal with limited data or the analyst's technical judgment in defining covariance kernels (Faes and Moens, 2019b).

Therefore, the choice of one approach or the other will depend on both the available data resources and the objective of the study. Given limited information, users should ask themselves which approach will provide the most meaningful results. The main factors that the authors consider relevant to make this decision are summarized in the comparison Table 2, based on the previous discussion. In geotechnical studies, this is a matter of considerable concern. First, the nature of uncertainty in soil properties lies in spatial variability and lack of knowledge, as opposed to, for example, manufacturing processes where there is a high random component. Thus, if the purpose is to quantify the uncertainty associated with the response of interest, the choice of an interval-based approach could provide results that are more consistent with the information measured in the field. On the other hand, if the purpose of the study is to update previous knowledge and sufficient information is available, then a Bayesian approach may be more appropriate for decision making. However, if the information is limited, an interval approach for inverse uncertainty quantification will provide a more objective uncertainty analysis at the cost of providing only worst-case information to the users (Faes et al., 2019). Second, it is important to note that one of the main features of the interval-based approach is its emphasis on extreme events for critical engineering decisions. This feature makes this method more suitable in cases where complete knowledge of the response of interest is not desired, but rather information is needed for an early stage of design. For detailed numerical comparisons between random field approaches and interval-based methods, readers are referred to the work of Beer et al. (2013b) and Chen et al. (2020).

Table 2
Systematic comparison of random fields and fuzzy fields.

Aspect	Random fields	Fuzzy fields
Amount of data	Requires significant amounts of informative data to accurately capture the nature of the uncertain property (Sharma et al., 2021)	Requires less data to objectively describe the nature of the uncertain property (Chen et al., 2020), can handle vagueness and scarcity of data (Verhaeghe et al., 2013; Schietzold et al., 2019)
Spatial properties	Usually assumes stationarity and statistical properties remain constant over the study area (Cho, 2012). Non- stationary requires space-dependent correlation functions (Liu et al., 2017a)	Does not assume stationarity, can handle spatial dependencies (Faes and Moens, 2017) due to the construction of the basis functions (Faes and Moens, 2020)
Purpose of the study	From any statistical property (Griffiths and Fenton, 1997; Srivastava et al., 2010), to the probability of failure (Valdebenito et al., 2019) and sensitivity analysis (Sudret, 2008)	Often limited to study worst-case scenarios (Degrauwe et al., 2010) by computing the extreme values of the response (Feng et al., 2022), and sensitivity analysis of the bounds of the uncertain parameters (Beer et al., 2013b)
Type of information obtained	Full probabilistic descriptions of the response of interest (Santoso et al., 2010, 2011)	Spatial distribution of the bounds on the epistemic uncertainty including their spatial dependence (Faes and Moens, 2019a), as well as a measure of the sensitivity concerning input uncertainty (Beer et al., 2013b)
Model parameters and assumptions	Distribution types and families of (auto)correlation functions (Srivastava et al., 2010)	Bounds of the uncertainty property at the control points (Faes and Moens, 2017). Power p to construct the basis functions (van Mierlo et al., 2021)
Uncertainty propagation approaches	Monte Carlo simulation, perturbation methods, spectral methods, and sampling methods (Stefanou, 2009), as well as geostatistical methods (Phoon et al., 2004) are commonly used to propagate uncertainty	Fuzzy analysis (Möller and Beer, 2004), interval arithmetic (Moore, 1966), parallel Bayesian global optimization (Dang et al., 2020), and interval analysis (Faes and Moens, 2019a) are often used to propagate uncertainty
Interpretability of results	Full probabilistic description of subjective knowledge, reliability and probability of failure of the system (Vanmarcke, 1983)	Results can be interpreted in terms of interval estimates with their sensitivity, providing insight into the degree of uncertainty (Moens and Vandepitte, 2005; Verhaeghe et al., 2013). Helps to identify which parameters need further measurement to reduce uncertainty (Beer et al., 2013b)

5. Conclusions

This paper presents a methodology to estimate the responses of a confined saturated seepage problem using fuzzy fields to capture the spatial uncertainty in hydraulic conductivity. The approach is formulated to propagate the uncertain hydraulic conductivity through the α-level optimization scheme. In particular, the subsequent challenges are addressed: (1) to include spatial dependencies in the horizontal and vertical hydraulic conductivity, and (2) to propose an approach for seepage analysis that allows scarce field measurements to be incorporated.

The results in terms of flow rate, uplift force, and exit gradient exhibit that fuzzy fields are useful for spatial uncertainty quantification under limited data. Fuzzy fields simplify the characterization of uncertain input parameters, requiring only the boundaries of each variable and (subjectively defined) membership functions. This flexibility allows users to define the location and number of control points based on available data, allowing spatial dependencies to be incorporated into the analysis. Despite the limited number of observations considered available for the illustrative example, it was found that it is possible to construct the fuzzy field and gain an understanding of the degree of uncertainty of the seepage responses of total flow, uplift force, and exit gradient. As a result, even when limited uncertain information is available, it can be considered for seepage analysis. Therefore, fuzzy fields offer an attractive alternative to classical probabilistic seepage analysis. Furthermore, fuzzy field analysis must be understood as a way to perform sensitivity analysis. The response concerning the exit gradient showed the highest variation with respect to the deterministic analysis, being the most sensitive response to the variability present in hydraulic conductivity. Conversely, the uplift force was the least variant with respect to the uncertainty considered in hydraulic conductivity. The reason for that behavior was its strong dependence on the upstream head, which was considered deterministic.

Regarding the sensitivity analysis, the most extreme values of the responses analyzed were obtained with a value of $p = 2$. The aforementioned behavior is relevant for design proposes and stability studies. Moreover, particular attention regarding the selection of the parameter p should be made to avoid the effect of local influences. However, despite variations in the analyzed responses with respect to the value of p considered, the differences among them were not significant for the critical values (right tail of the membership functions). This implies that the selection of the value of p has a minor influence on the extreme responses, with this being the only parameter to be selected for the construction of the fuzzy field. This is an advantage over probabilistic approaches which often require the assumption of marginal distributions and correlation functions of the input data. Therefore, the fuzzy field methodology presented in this study provides an approach that requires few assumptions to deal with seepage analysis.

Nevertheless, the exhibited results should be regarded as an initial approximation of fuzzy field analysis for seepage problems. First, the sensitivity analysis performed in this study must be treated as a preliminary approach to understanding the spatial dependence structure of soil hydraulic conductivity. Forthcoming studies steps will explore challenges such as improved strategies to propagate uncertainty when fuzzy fields are involved, and the gradient of the basis functions and its relation to the finite element mesh to avoid convergence studies. Another focus of future studies will be the inclusion of machine learning techniques to define the dependency structure of the data at control points and implement fuzzy fields based on real data for more complex systems and other types of analyses. For example, to extend the fuzzy field framework to unsaturated seepage analysis, considering soil-water characteristic curves to incorporate uncertainty in hydraulic conductivity, and employing efficient strategies to overcome the associated numerical cost.

CRediT authorship contribution statement

Nataly A. Manque: Writing – original draft, Methodology, Investigation, Formal analysis. **Kok-Kwang Phoon:** Writing – review & editing, Validation, Methodology. **Yong Liu:** Writing – review & editing, Validation, Methodology. **Marcos A. Valdebenito:** Writing – review & editing, Validation, Supervision, Methodology, Conceptualization. **Matthias G.R. Faes:** Writing – review & editing, Validation, Supervision, Methodology, Conceptualization.

Declaration of competing interest

The authors declare that they have no known competing financial interests or personal relationships that could have appeared to influence the work reported in this paper.

References

Abd-Elaty, I., Zelenakova, M., Straface, S., Vranayová, Z., Abu-hashim, M., 2019. Integrated modelling for groundwater contamination from polluted streams using new protection process techniques. Water 11, 2321.
Ahmed, A.A., 2009. Stochastic analysis of free surface flow through earth dams. Comput. Geotech. 36, 1186–1190.
Ahmed, S., Jayakumar, R., Salih, A., 2008. Groundwater Dynamics in Hard Rock Aquifers Sustainable Management and Optimal Monitoring Network Design. Springer.
Alrdadi, R., Meylan, M.H., 2022. Modelling water flow through railway ballast with random permeability and a free boundary. Appl. Math. Model. 103, 36–50.
Arshad, M., Nazir, M.S., O'Kelly, B.C., 2020. Evolution of hydraulic conductivity models for sandy soils. Proc. Inst. Civil Eng.-Geotech. Eng. 173, 97–114.
Baroni, G., Zink, M., Kumar, R., Samaniego, L., Attinger, S., 2017. Effects of uncertainty in soil properties on simulated hydrological states and fluxes at different spatio-temporal scales. Hydrol. Earth Syst. Sci. 21, 2301–2320.
Beer, M., Ferson, S., Kreinovich, V., 2013a. Imprecise probabilities in engineering analyses. Mech. Syst. Signal Process. 37, 4–29.
Beer, M., Zhang, Y., Quek, S.T., Phoon, K.K., 2013b. Reliability analysis with scarce information: comparing alternative approaches in a geotechnical engineering context. Struct. Saf. 41, 1–10.
Bianchi, D., Gallipoli, D., Bovolenta, R., Leoni, M., 2022. Analysis of unsaturated seepage in infinite slopes by means of horizontal ground infiltration models. Geotechnique 74 (8), 820–828.
Cai, J.S., Yeh, T.C.J., Yan, E.C., Hao, Y.H., Huang, S.Y., Wen, J.C., 2017. Uncertainty of rainfall- induced landslides considering spatial variability of parameters. Comput. Geotech. 87, 149–162.
Cho, S.E., 2012. Probabilistic analysis of seepage that considers the spatial variability of permeability for an embankment on soil foundation. Eng. Geol. 133–134, 30–39.
Chen, Z.-Y., Imholz, M., Li, L., Faes, M., Moens, D., 2020. Transient landing dynamics analysis for a lunar lander with random and interval fields. Appl. Math. Model. 88, 827–851.
Dane, J.H., Topp, G.C. (Eds.), 2002. Methods of Soil Analysis. Soil Sci. Soc. Am.
Dang, C., Wei, P., Faes, M.G.R., Valdebenito, M.A., Beer, M., 2020. Interval uncertainty propagation by a parallel Bayesian global optimization method. Appl. Math. Model. 108, 220–235.
De Mulder, W., Moens, D., Vandepitte, D., 2012. Modeling uncertainty in the context of finite element models with distance-based interpolation. In: Uncertainties 2012, Sao Paulo, Brazil.
Degrauwe, D., Lombaert, G., Roeck, G.D., 2010. Improving interval analysis in finite element calculations by means of affine arithmetic. Comput. Struct. 88, 247–254.
Deng, Y.F., Tang, A.M., Cui, Y.J., Li, X.L., 2011. Study on the hydraulic conductivity of Boom clay. Can. Geotech. J. 48, 1461–1470.
Der Kiureghian, A., Ke, J.B., 1988. The stochastic finite element method in structural reliability. Probabilist. Eng. Mech. 3, 83–91.
Ding, S., Shao, G., Huang, Y., Shi, H., 2021. The superconvergence gradient recovery method for linear finite element method with polygons. Int. J. Numer. Methods Eng. 122, 4154–4171.
Elhakim, A.F., 2016. Estimation of soil permeability. Alex. Eng. J. 55, 2631–2638.
Eslami, A., Molaabasi, H., Eslami, M.M., Moshfeghi, S., 2019. Piezocone Penetration Test Application in Foundation Engineering - CPT and CPTu. Elsevier Sci. Technol.
Faes, M., Broggi, M., Patelli, E., Govers, Y., Mottershead, J., Beer, M., Moens, D., 2019. A Multivariate Interval Approach for Inverse Uncertainty Quantification with Limited Experimental Data, vol. 118. Mech. Syst. Signal Proc., pp. 534–548

Faes, M., Moens, D., 2017. Identification and quantification of spatial interval uncertainty in numerical models. Comput. Struct. 192, 16–33.
Faes, M., Moens, D., 2019a. Imprecise random field analysis with parametrized kernel functions. Mech. Syst. Signal Process. 134, 106334.
Faes, M., Moens, D., 2019b. Recent trends in the modeling and quantification of non-probabilistic uncertainty. Arch. Comput. Methods Eng. 27, 633–671.
Faes, M., Moens, D., 2020. On auto- and cross-interdependence in interval field finite element analysis. Int. J. Numer. Methods Eng. 121, 2033–2050.
Faes, M.G., Broggi, M., Chen, G., Phoon, K.K., Beer, M., 2022. Distribution-free p-box processes based on translation theory: definition and simulation. Probabilist. Eng. Mech. 69, 103287.
Fanchi, J.R., 2010. 4 - porosity and permeability. In: Fanchi, J.R. (Ed.), Integrated Reservoir Asset Management. Gulf Prof. Publ., Boston, pp. 49–69.
Feng, C., Faes, M., Broggi, M., Dang, C., Yang, J., Zheng, Z., Beer, M., 2022. Application of interval field method to the stability analysis of slopes in presence of uncertainties. Comput. Geotech., 105060
Feng, S., Vardanega, P.J., 2019. A database of saturated hydraulic conductivity of fine-grained soils: probability density functions. Georisk 13, 255–261.
Gong, W., Zhao, C., Juang, C.H., Tang, H., Wang, H., Hu, X., 2020. Stratigraphic uncertainty modelling with random field approach. Comput. Geotech. 125, 103681.
Götz, M., Graf, W., Kaliske, M., 2019. Enhanced uncertain structural analysis with time- and spatial-dependent (functional) fuzzy results. Mech. Syst. Signal Process. 119, 23–38.
Griffiths, D.V., Fenton, G.A., 1993. Seepage beneath water retaining structures founded on spatially random soil. Geotechnique 43, 577–587.
Griffiths, D.V., Fenton, G.A., 1997. Three-dimensional seepage through spatially random soil. J. Geotech. Geoenviron. Eng. 123, 153–160.
Griffiths, D.V., Fenton, G.A., 1998. Probabilistic analysis of exit gradients due to steady seepage. J. Geotech. Geoenviron. Eng. 124, 789–797.
Gu, X., Wang, L., Ou, Q., Zhang, W., 2023. Efficient stochastic analysis of unsaturated slopes subjected to various rainfall intensities and patterns. Geosci. Front. 14, 101490.
Guan, Z., Wang, Y., 2022. CPT-based probabilistic liquefaction assessment considering soil spatial variability, interpolation uncertainty and model uncertainty. Comput. Geotech. 141, 104504.
Hager, W.H., Schleiss, A.J., Boes, R.M., Pfister, M., 2020. Hydraulic Engineering of Dams. CRC Press.
Hanss, M., 2005. Applied Fuzzy Arithmetic. Springer, Berlin Heidelberg.
He, L.P., Huang, H.Z., Du, L., Zhang, X.D., Miao, Q., 2007. A review of possibilistic approaches to reliability analysis and optimization in engineering design. In: Human-Computer Interaction. HCI Applications and Services. Springer, Berlin Heidelberg, pp. 1075–1084.
Hekmatzadeh, A.A., Zarei, F., Johari, A., Haghighi, A.T., 2018. Reliability analysis of stability against piping and sliding in diversion dams, considering four cutoff wall configurations. Comput. Geotech. 98, 217–231.
Hesse, F., Müller, S., Attinger, S., 2024. Data-driven estimates for the geostatistical characterization of subsurface hydraulic properties. Hydrol. Earth Syst. Sci. 28, 357–374.
Huang, M., Jia, C.Q., 2009. Strength reduction FEM in stability analysis of soil slopes subjected to transient unsaturated seepage. Comput. Geotech. 36, 93–101.
Imholz, M., Faes, M., Vandepitte, D., Moens, D., 2020. Robust uncertainty quantification in structural dynamics under scarce experimental modal data: a Bayesian-interval approach. J. Sound Vib. 467, 114983.
Jiang, S.H., Huang, J., Griffiths, D., Deng, Z.P., 2022. Advances in reliability and risk analyses of slopes in spatially variable soils: a state-of-the-art review. Comput. Geotech. 141, 104498.
Jie, Y.X., Fu, X.D., Deng, G., 2013. Treatment of transitional element with the Monte Carlo method for FEM-based seepage analysis. Comput. Geotech. 52, 1–6.
Kennedy, J., Eberhart, R., 1995. Particle swarm optimization. In: Proceedings of ICNN'95- International Conference on Neural Networks. IEEE, Perth, WA, Australia, pp. 1942–1948.
Le, T.M.H., Gallipoli, D., Sanchez, M., Wheeler, S.J., 2011. Stochastic analysis of unsaturated seepage through randomly heterogeneous earth embankments. Int. J. Numer. Anal. Methods GeoMech. 36, 1056–1076.
Li, G., Shen, Z., Yang, C., 2020. A simplified calculation method of seepage flux for slope-wall rock-fill dams with a horizontal blanket. Appl. Sci. 10, 3848.
Lin, H., 2010. Earth's critical zone and hydropedology: concepts, characteristics, and advances. Hydrol. Earth Syst. Sci. 14, 25–45.
Liu, K., Vardon, P.J., Hicks, M.A., 2017b. Probabilistic analysis of seepage for internal stability of earth embankments. Environ. Geotech. 6, 294–306.
Liu, L.L., Cheng, Y.M., Jiang, S.H., Zhang, S.H., Wang, X.M., Wu, Z.H., 2017a. Effects of spatial autocorrelation structure of permeability on seepage through an embankment on a soil foundation. Comput. Geotech. 87, 62–75.
Lu, Z., Zhang, D., 2007. Stochastic simulations for flow in nonstationary randomly heterogeneous porous media using a KL-based moment-equation approach. Multiscale Model. Simul. 6, 228–245.
Mansuri, B., Salmasi, F., Oghati, B., 2014. Effect of location and angle of cutoff wall on uplift pressure in diversion dam. Geotech. Geol. Eng. 32, 1165–1173.
Meyer, W., Schuster, R.L., Sabol, M.A., 1994. Potential for seepage erosion of landslide dam. J. Geotech. Eng. 120, 1211–1229.
Moens, D., Vandepitte, D., 2005. A survey of non-probabilistic uncertainty treatment in finite element analysis. Comput. Methods Appl. Mech. Eng. 194, 1527–1555.
Moens, D., Vandepitte, D., 2007. Interval sensitivity theory and its application to frequency response envelope analysis of uncertain structures. Comput. Methods Appl. Mech. Eng. 196, 2486–2496.
Möller, B., Beer, M., 2004. Fuzzy Randomness. Springer, Berlin Heidelberg.
Möller, B., Graf, W., Beer, M., 2000. Fuzzy structural analysis using α-level optimization. Comput. Mech. 26, 547–565.
Montoya-Noguera, S., Zhao, T., Hu, Y., Wang, Y., Phoon, K.K., 2019. Simulation of non- stationary non-Gaussian random fields from sparse measurements using Bayesian compressive sampling and Karhunen-Loève expansion. Struct. Saf. 79, 66–79.
Moore, R.T., 1966. Interval Analysis. Prentice Hall, Englewood Cliffs.
Norouzi, R., Salmasi, F., Arvanaghi, H., 2020. Uplift pressure and hydraulic gradient in Sabalan Dam. Appl. Water Sci. 10.
Phoon, K.K., 2019. Editorial: flow and transport in porous media in the face of uncertainty, part i. Environ. Geotech. 6, 186–187.
Phoon, K.K., Kulhawy, F.H., 1999. Characterization of geotechnical variability. Can. Geotech. J. 36, 612–624.
Phoon, K.K., Quek, S.T., An, P., 2004. Geostatistical analysis of cone penetration test (CPT) sounding using the modified Bartlett test. Can. Geotech. J. 41, 356–365.
Phoon, K.K., Santoso, A., Quek, S.T., 2010. Probabilistic analysis of soil-water characteristic curves. J. Geotech. Geoenviron. Eng. 136, 445–455.
Prakash, A., Hazra, B., S, S., 2021. Probabilistic analysis of soil-water characteristic curve using limited data. Appl. Math. Model. 89, 752–770.
Previati, G., Gobbi, M., Ballo, F., 2019. A study on the stress gradient reconstruction in finite elements problems with application of radial basis function networks. Meccanica 54, 47–70.
Richards, L.A., 1931. Capillary conduction of liquids through porous mediums. Phys. 1, 318–333.
Santoso, A., Phoon, K.K., Quek, S.T., 2010. Flow of water through spatially heterogeneous soil. In: Li, J.C.C., Lin, M.-L. (Eds.), Seventeenth Southeast Asian Geotechnical Conference: Geo-Engineering for Natural Hazard Mitigation and Sustainable Development. Taiwan Geotechnical Society, Taiwan, pp. 249–253.
Santoso, A.M., Phoon, K.K., Quek, S.T., 2011. Effects of soil spatial variability on rainfall-induced landslides. Comput. Struct. 89, 893–900.
Schietzold, F.N., Schmidt, A., Dannert, M.M., et al., 2019. Development of fuzzy probability based random fields for the numerical structural design. GAMM-Mitteilungen 42, e201900004.
Sharma, A., Hazra, B., Sekharan, S., 2021. Stochastic seepage and slope stability analysis using vine-copula based multivariate random field approach: consideration to non-Gaussian spatial and cross-dependence structure of hydraulic parameters. Comput. Geotech. 130, 103918.
Shedid, S.A., 2019. Vertical-horizontal permeability correlations using coring data. Egypt. J. Petrol. 28, 97–101.
Singh, V.K., Kumar, D., Kashyap, P., Singh, P.K., Kumar, A., Singh, S.K., 2020. Modelling of soil permeability using different data driven algorithms based on physical properties of soil. J. Hydrol. 580, 124223.
Sofi, A., Romeo, E., 2016. A novel Interval Finite Element Method based on the improved interval analysis. Comput. Methods Appl. Mech. Eng. 311, 671–697.
Sofi, A., Romeo, E., Barrera, O., Cocks, A., 2019. An interval finite element method for the analysis of structures with spatially varying uncertainties. Adv. Eng. Softw. 128, 1–19.
Srivastava, A., Babu, G.S., Haldar, S., 2010. Influence of spatial variability of permeability property on steady state seepage flow and slope stability analysis. Eng. Geol. 110, 93–101.
Stefanou, G., 2009. The stochastic finite element method: past, present and future. Comput. Methods Appl. Mech. Eng. 93, 964–979.
Sudret, B., 2008. Global sensitivity analysis using polynomial chaos expansions. Reliab. Eng. Syst. Saf. 198, 1031–1051.
Teng, J., Kou, J., Zhang, S., Sheng, D., 2019. Evaluating the influence of specimen preparation on saturated hydraulic conductivity using nuclear magnetic resonance technology. Vadose Zone J. 18, 1–7.
Terzaghi, K., Peck, R.B., 1967. Soil Mechanics in Engineering Practice. Wiley.
Valdebenito, M.A., Hernández, H.B., Jensen, H.A., 2019. Probability sensitivity estimation of linear stochastic finite element models applying Line Sampling. Struct. Saf. 81, 101868.
van Mierlo, C., Faes, M.G., Moens, D., 2021. Inhomogeneous interval fields based on scaled inverse distance weighting interpolation. Comput. Methods Appl. Mech. Eng. 373, 113542.
Vanmarcke, E., 1983. Random Fields, Analysis and Synthesis. MIT Press.
Verhaeghe, W., De Munck, M., Desmet, W., Vandepitte, D., Moens, D., 2010. A fuzzy finite element analysis technique for structural static analysis based on interval fields. In: Proceedings of the 4th International Workshop on Reliable Engineering Computing. Research Publishing Services, Singapore, pp. 117–128.
Verhaeghe, W., Desmet, W., Vandepitte, D., Joris, I., Seuntjens, P., Moens, D., 2013. Application of interval fields for uncertainty modeling in a geohydrological case. In: Computational Methods in Stochastic Dynamics. Springer, Netherlands, pp. 131–147.
Wang, C., 2021. Reliability-based design of lining structures for underground space against water seepage. Undergr. Space 6, 290–299.
Wang, R.H., Sun, P.G., Li, D.Q., Tyagi, A., Liu, Y., 2021. Three-dimensional seepage investigation of riverside tunnel construction considering heterogeneous

permeability. ASCE-ASME J. Risk Uncertain. Eng. Syst. Part A Civ. Eng. 7.
Whitlow, R., 2000. Basic Soil Mechanics. Pearson Education (US).
Xiang, J., Scanlon, B., Mullican, W., Chen, L., Goldsmith, R., 1997. A multistep constant-head borehole test to determine field saturated hydraulic conductivity of layered soils. Adv. Water Resour. 20, 45–57.
Zadeh, L., 1965. Fuzzy sets. Inf. Control 8 (3), 338–353.
Zeng, Z., Cui, Y.J., Talandier, J., 2020. Evaluating the influence of soil plasticity on hydraulic conductivity based on a general capillary model. Eng. Geol. 278, 105826.
Zhai, Q., Rahardjo, H., 2013. Quantification of uncertainties in soil–water characteristic curve associated with fitting parameters. Eng. Geol. 163, 144–152.
Zhang, D., Nguang, S.K., Shu, L., Qiu, D., 2022. Multiple fuzzy parameters nonlinear seepage model for shale gas reservoirs. Int. J. Fuzzy Syst. 24, 2845–2857.
Zhang, D., Shu, L., Li, S., 2020. Fuzzy structural element method for solving fuzzy dual medium seepage model in reservoir. Soft Comput. 24, 16097–16110.
Zienkiewicz, O.C., 2000. The Finite Element Method. Butterworth-Heinemann.

Nataly A. Manque is currently a PhD student at the Chair for Reliability Engineering, TU Dortmund University, Germany. She received her BSc degree in Civil Engineering from the University of La Frontera, Chile in 2020 and her MSc degree in Civil Engineering from the Adolfo Ibáñez University, Chile in 2022. Her research interests include geotechnical uncertainty analysis under limited data, interval and fuzzy fields analysis, reduced-order models and isogeometric analysis.